In Transreactions in Condensation Polymers, Ed. S. Fakirov Wiley VCH, N.Y 1999

Chapter 6

Inhibition of Transreactions in Condensation Polymers

N. R. James, S. S. Mahajan, S. Sivaram

1. Introduction

1.1. *Polymer blends*

There has been tremendous commercial and scientific interest in polymer blends and alloys over the last several years [1]. The terms "blends" and "alloys" have become almost indistinguishable in industry parlance, possibly because of the convenience of semantically equating the two concepts. By strict definition there is a difference, although the basic goal of each is identical, which is to combine two or more polymers and thus make available the best properties of each polymer in a single material with an optimised cost and performance. The difference is that a blend is essentially a mechanical mixture, whereas an alloy is produced by achieving mixing of the polymers at a molecular level in a chemical reactor or extruder.

1.1.1. *Compatibility in polymer blends*

Few polymers form truly miscible blends characterised by a single glass transition temperature (T_g) and homogeneity on the 5–10 nm scale [2]. Miscibility in these systems is attributed to the presence of specific interactions, such as acid–base or ion–dipole, hydrogen bonding and transition metal complexation [3–6]. The majority of the blends are immiscible and possess a phase separated morphology. The physical properties of such blends are limited by the large domain size, poor interfacial adhesion, and the

tendency to form unstable morphologies. Heterogeneous blends of technological importance are termed "compatible" [7,8]. The differences between miscible, immiscible and compatibilised blends is illustrated in Figure 1.

Miscible blends are thermodynamically stable, molecular-level mixtures. Immiscible blends are separated into macroscopic phases with minimal interfacial adhesion and unstable morphologies. Compatibilised blends are also macro-phase separated. However, the presence of interfacial agents or chemical bonds stabilises the morphology and increases interfacial adhesion. In such blends, satisfactory physical and mechanical properties are related to the presence of a finely dispersed phase and resistance to gross phase segregation.

The presence of a compatibilising agent permits the blending of otherwise incompatible polymers to yield blends or alloys with unique properties, generally not attainable from the individual components. Compatibility is promoted through block and graft copolymers possessing segments with chemical structures or solubility parameters which are similar to those of the polymers being blended. The copolymer may be preformed and added

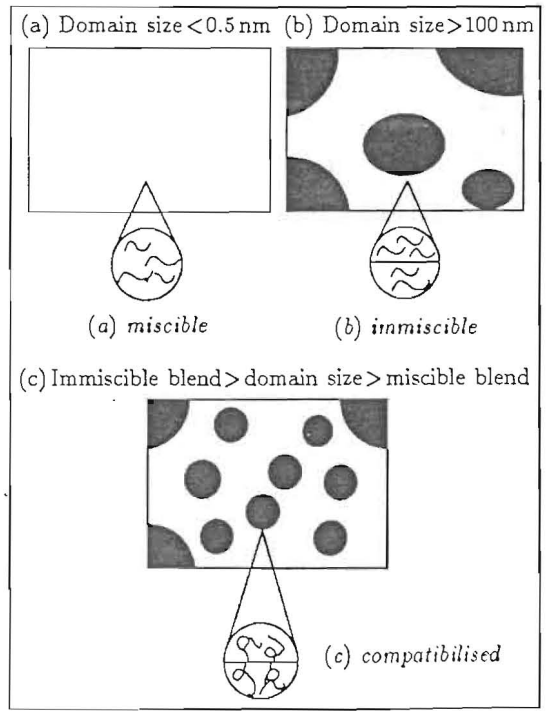

Figure 1. Differences between miscible, immiscible, and compatibilised blends [13]

to the mixture of polymers or formed *in situ* by reaction between co-reactive functional groups on the polymers. The compatibilising agent acts as a polymeric surfactant, which lowers surface tension and promotes interfacial adhesion between the dispersed and matrix polymer phases. Compatibilisation of polymer blends through reactions during compounding is becoming increasingly important and is known as reactive compatibilisation [9–13].

1.2. *Reactive compatibilisation*

Reactive compounding in a twin screw extruder usually involves highly reactive functional groups, which are unstable under processing conditions. The inherent functionality present in end-groups of the polymer pairs as well as polymer–polymer cross reactions are often exploited. Some examples of common compatibilising reactions between functional blend constituents are shown in Figure 2.

Compatibility is promoted by the presence of functional groups which undergo chemical reaction. A segment of a compatibilising agent containing reactive functionality (X) compatibilises a polymer having a different structure as well as a different solubility parameter but having a co-reactive functionality (Y).

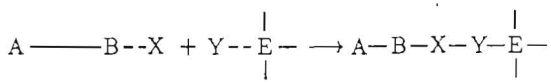

The resultant graft or block copolymer, prepared *in situ* from a functionalised polymer containing pendant or terminal functionality is a compatibilising agent for unfunctionalised A and E polymers.

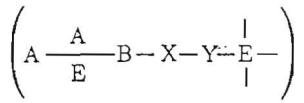

The compatibilising agent functions as an organic surfactant and is thought to concentrate at the interface of two incompatible polymer phases and act as an emulsifiers, reducing interfacial tension. It promotes adhesion also through interpenetration and entanglements (see also Chapter 10).

1.3. *Transreaction during melt-blending*

During the last few years, research efforts have been directed towards the development of blends from existing polymers by moving the chemistry from reaction vessels into processing equipment. This is often referred to as reactive processing. The reactions occurring during melt-blending can modify the chemical structure and improve compatibility between polymers which are otherwise immiscible [20]. This approach is particularly attractive in the case of polycondensates, which usually contain reactive functional

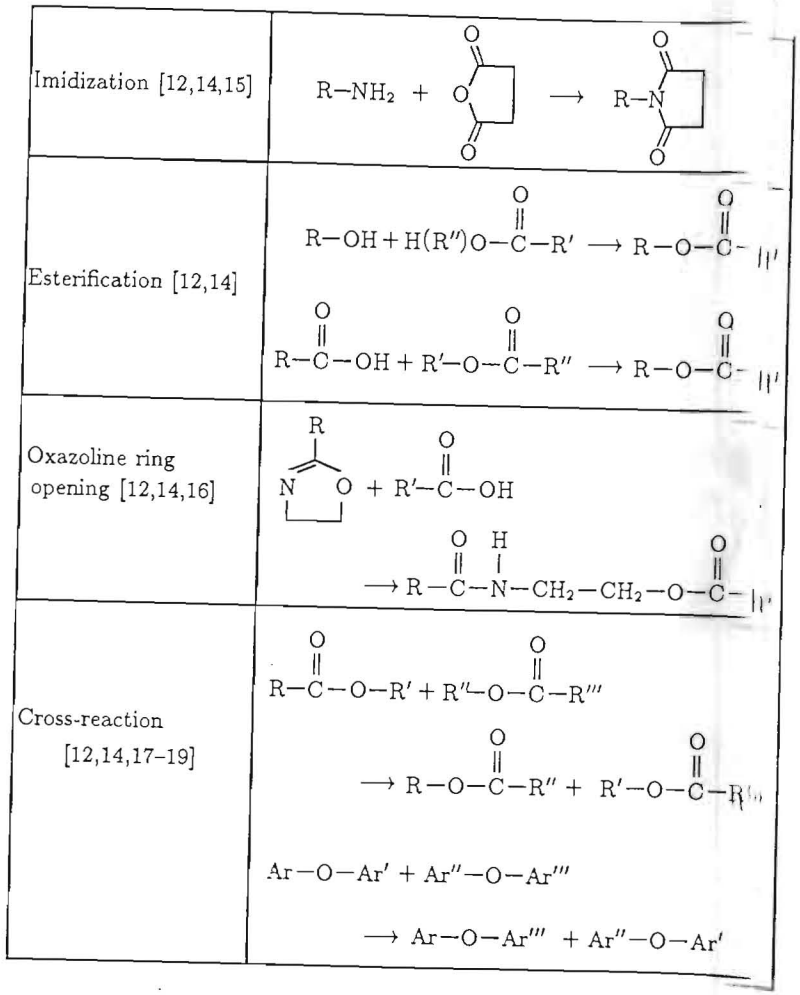

Figure 2. Examples of common compatibilised reactions between functional blend constituents [13]

groups along the backbone and can undergo exchange reactions under suitable reaction conditions. Reactive blending can be applied to many polycondensates, opening the possibility for the preparation of a number of new materials by the direct combination of two or more polymers in processing machines such as extruders. This processing technology has many desirable features. It is complementary to polymerisation processes, has a high flexibility and versatility, requires lower capital investment, and is

Table 1. Types of chemical reactions performed by reactive extrusion

Type	Description
Bulk polymerisation	Preparation of high molecular weight polymer from monomer or low molecular weight prepolymer, or from mixture of monomers or monomer and prepolymer
Graft reaction	Formation of grafted polymer or copolymer from reaction of polymer and monomer
Interchain copolymer formation	Reaction of two or more polymers to form random, graft, or block copolymer through either ionic or covalent bonds
Coupling/crosslinking reactions	Reaction of polymer with polyfunctional coupling or branching agent to build molecular weight by chain extension or branching, or reaction of polymer with condensing agent to build molecular weight by chain extension, or reaction of polymer with crosslinking agent to build melt viscosity by crosslinking
Controlled degradation	Controlled molecular weight degradation of high molecular weight polymer (controlled rheology), or controlled degradation to monomer
Functionalisation/ functional-group modification	Introduction of functional groups into polymer backbone, end-group, or side chain, or modification of existing functional groups

more environmentally friendly. The types of chemical reactions which are performed by reactive extrusion may be divided into different categories as described in Table 1 (see also Chapter 7).

1.3.1. *Interchain copolymer formation*

Interchain copolymer formation by reactive extrusion is particularly useful for compatibilisation of immiscible polymer blends. Interchain copolymer formation may be defined as reaction of two (or more) polymers to form copolymer. Most of the condensation polymers have nucleophilic end-groups, such as carboxylic acid, amine, and hydroxyl groups. These nucleophilic end-groups can form covalent bonds with suitable electrophilic functionality leading to copolymer formation when a suitable electrophilic group is attached to a second polymer. The kinds of electrophilic functionalities that can form covalent bonds across a phase interface within the time constraints of an extruder are cyclic anhydride, epoxide, oxazoline, isocyanate, and carbodiimide. Kotliar [21] has reviewed the interchange reactions involving condensation polymers such as polyesters and polyamides.

The various types of interchange reactions in polyesters are

Intermolecular alcoholysis

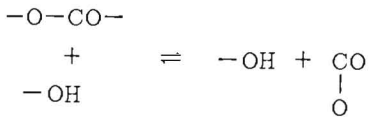

Intermolecular acidolysis

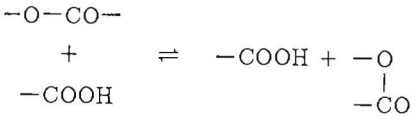

Transesterification

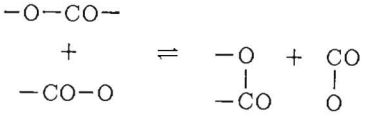

Interchange reactions in condensation polymerisation of polyesters and polyamides have been studied extensively [22–26]. It is also known that such reactions occur during melt processing of these polymers and form copolymers which change from block to random structures with time. Very little information is available in the open and patent literature about interchange reactions in polyamide/polyamide blends. Flory [22] suggests that aminolysis occurs with the possibility of amide exchange in polyamide melts. These reactions are

Intermolecular acidolysis

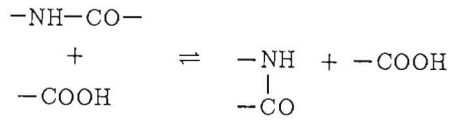

Intermolecular aminolysis

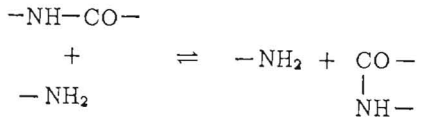

Intermolecular amidolysis

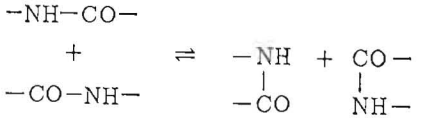

Blends of nylon 6 with nylon 6,6 are commercially important since they can give certain desirable properties, such as low-temperature toughness, increased flexibility, *etc.* Recent patents describe the preparation and properties of these blends [27,28]. According to these patents nylon 6 and nylon

6,6 homopolymers undergo facile interchange reactions in the presence of certain catalysts to yield random copolymers during the processing. Verma *et al.* investigated [29] the melt blending of nylon 6 with nylon 6,6 without the addition of any external catalyst and found that little reaction occurs, as deduced from two distinct melting peaks of the homopolymers in the blend.

Prevention of exchange reactions and of fast exchange reactions are both quite important. However, not much work has been done in this field. Hence there is a need to study the reaction kinetics thoroughly to understand the mechanism of transamidation reactions. The chemical processes for interchain copolymer formation in extruder reactors are summarised in Table 2. The types of copolymers formed are illustrated through the reaction of two polymers, namely, AAAAA and BBBBB.

Interchain copolymer formation through chain cleavage followed by recombination is not a very useful process, as resulting copolymers are obtained as mixtures having broad molecular weight distributions. In the early

Table 2. Chemical processes for interchain copolymer formation in extruder reactors

Process	Type of copolymer obtained
1.Chain cleavage/recombination	Block and random AAAAABBBBBB + AABBBBBAAAAA + AABBAAABBB, *etc.*
2.End-group of 1st polymer + end-group of 2nd polymer	Block AAAAABBBBB
3.End-group of 1st polymer + pendant functionality of 2nd polymer	Graft A BBBBB A A-BBBBB A
4.Covalent crosslinking: pendant functionality of 1st polymer + pendant functionality of 2nd polymer or Main chain of 1st polymer + main chain of 2nd polymer	Graft (crosslinked network) Graft (crosslinked network)
5.Ionic bond formation	Usually graft (usually crosslinked) A B A—B A B A—B A B

stages of such a process, block copolymers may predominate over random copolymer; however, such block copolymers have molecular weights less than the sum of the homopolymers and they may not be effective compatibilisers compared with the block copolymers formed by end-group/end-group reaction. Block or graft copolymers are formed in extruder reactors through reaction between functionalised end-groups of two different polymers. Because the probability of end-groups reacting within the extruder time scale is low, highly reactive functionality is necessary on the two substrate polymers.

Interchain copolymer formation by either covalent or ionic crosslinking is also possible in extruder reactors. In covalent crosslinking, pendant functionality of one polymer reacts with pendant functionalities of a second polymer to form a covalent bond. In ionic crosslinking, acidic groups, such as carboxylic, sulfonic, or phosphoric acid are present on both polymers and are at least partially neutralised by a metal cation, usually divalent, which may form a bridge between the two polymers being extruded. In some cases, polymers containing masked ionomers, chemical groups which form ionic species during the extrusion process, have been used to form copolymers during reactive extrusion. Use of masked ionomers may result in lower energy during extrusion processing since ionic self-association need not be overcome before interchain copolymer formation can occur.

2. Control of transesterification in polyester blends

2.1. *Introduction*

A fascinating feature of blends in the polyester family is the transreaction which is also known as transesterification. Ester exchange reactions have been reported to occur during extrusion of polyester blends [30–33]. As transesterification proceeds, blends convert first to block copolymers and finally to random copolymers. The resultant initial blocks and eventual random copolymers are expected to exhibit enhanced mutual miscibility over the original unreacted components. Transesterified copolymers may exhibit some advantages such as higher tensile strength in polycarbonate/polyarylate blends [34], but these blends display poor impact properties [35]. The extent of exchange reaction is a key variable with regard to the phase behaviour of a given blend.

There is an increasing interest in the understanding of the exchange reactions that take place in polymer blends between different functional groups involved in the mixtures of some polycondensation polymers. Of particular interest have been the industrially important blends based on polyester/polyester or polyester/polycarbonate. The chemical structure, and therefore the properties, of the resulting polymeric materials, are controlled by the relative rate and extent of several reactions which occur during the melt-blending. Transesterification makes it possible to obtain

copolymers with different levels of randomness and composition by changing the weight fraction of each mixed polymer and reaction conditions such as temperature and residence time.

Since ester exchange reactions affect mechanical properties, it is essential to control the extent of exchange reactions during melt-blending in order to achieve the desired properties. Devaux *et al.* found that residual polymerisation catalyst caused ester exchange reactions. Organophosphorus compounds, such as phosphites [36,37], phosphonates [38], and phosphates [39], have been used to inhibit ester exchange reaction in the molten state.

Cheung *et al.* have also proposed the inhibition of ester exchange reactions by organophosphates in a polyarylate/polycarbonate/poly(ethylene terephthalate) (PAr/PC/PET) ternary blend [40]. Control of processing conditions to minimise the extent of exchange reactions in the polycarbonate/polyarylate blends has been discussed by Mondragon and Nazabal [34]. The activity of a catalyst, either present as a residue from polymer synthesis or purposely added before blending, may play a role in controlling the chemical structure of the resultant product.

2.2. *Inhibitors for transreaction in polyester and polycarbonate blends*

2.2.1. *Organophosphite catalysts*

Molten polyesters can undergo transesterification during processing, resulting in chemical structures ranging from diblock copolymers with high molecular weight blocks, to multiblock copolymers with shorter and shorter segments, and eventually to random copolymers. Ester exchange reactions in polyester blends may lead to materials with poor mechanical properties. To inhibit or suppress transesterification, the use of organophosphites has been suggested in the patent and technical literature. The exact mechanism for the stabilising effect of the phosphite is unknown. Devaux *et al.* have found that organophosphite was useful to inhibit ester exchange reactions by forming an octahedral complex with residual catalysts which catalyse the transesterification reaction. They observed that phosphites, such as di-*n*-octadecyl phosphite, diphenyl phosphite and triphenyl phosphite were very effective in the inactivation of titanate catalyst residing in poly(butylene terephthalate) (PBT) after polymerisation. Triphenyl phosphite appeared to be the most effective inhibitor after an exchange of its phenol ligand by hydrolysis. Hydrolysis of triphenyl phosphite leads to diphenyl phosphite which upon further hydrolysis generates phosphoric aicd. This acid can tautomerise to phosphonic acid. According to Verhoeven [41], phosphonic acid is a possible titanate inhibitor. Cheung *et al.* [40] have reported the results of inhibiting the ester exchange reaction by organophosphites in a polyarylate/polycarbonate/poly(ethylene terephthalate) (PAr/PC/PET) ternary blend. According to them, the phosphites

appear to be transformed into phosphonates, which are effective inhibitors for the exchange reactions. Using solid-state ^{31}P NMR spectroscopy it was shown that for bis(2,4-di-t-butylphenyl)pentaerythritol diphosphite (Ultranox 624), a conversion of the phosphite group to phosphonate, *via* hydrolysis at high processing temperature, is a prerequisite for an effective inhibition of transesterification. This conversion occurs readily during melt compounding if the polymers are not completely dry. However, if rigorous drying is employed and phosphite conversion does not occur, then transesterification is not arrested.

The results indicate that the organophosphite may have reacted, with the moisture from the environment during extrusion through side-chain hydrolysis, been converted into the tricovalent phosphoric acid (H–O–P) and later tautomerised into the more stable pentacovalent form (H–P=O) as follows:

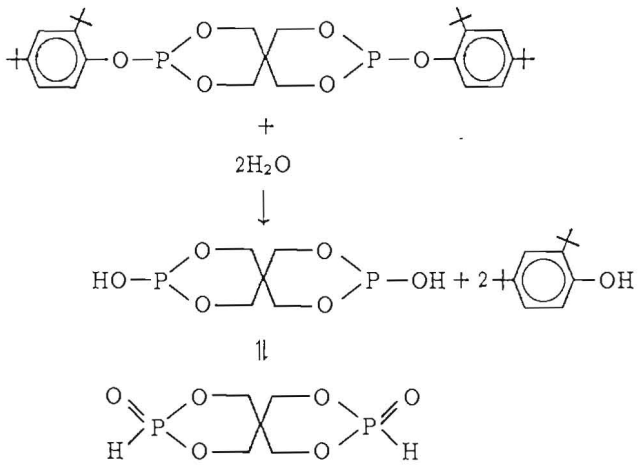

The carboxyl end-groups in PET can react with the diphosphite (Ultranox 624) and form phosphonic acid, which is subsequently transformed into a phosphonate, as follows:

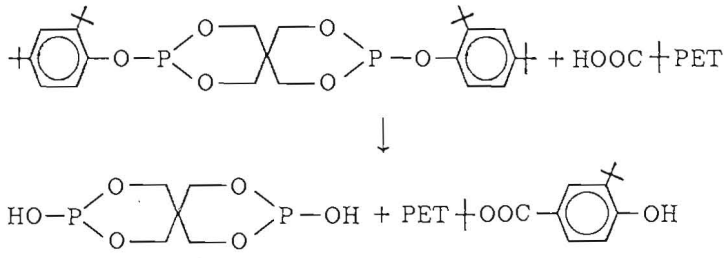

It was also found that the conversion of the diphosphite in Ultranox 624 occurs not only during the processing but also at room temperature and in tightly closed steel containers, albeit slowly. Thus, in a period of about one year of storage in steel containers, sufficient conversion of the previously ineffective inhibitor took place to bring about a substantial improvement in the effectiveness of Ultranox 624 in suppressing transesterification reactions in blends of PET and PBT with polyarylate and polycarbonate.

Differential scanning calorimetry (DSC) was employed to evaluate the effectiveness of the inhibitor. When an organophosphite is used to suppress the ester exchange reactions, it has been found that whenever the phosphite is converted into a phosphonate, there is little change in both the melting point and the heat of fusion of PET during prolonged exposure to high temperature in the blends. The addition of an organophosphate to the PAr/PC/PET ternary blend effectively retards ester exchange reactions when the extrusion temperature is up to 280°C. Beyond 280°C, the phosphite stabilised blend shows signs of instability. The criterion for stability is the retention of the cold crystallisation exotherm and the heat of fusion of PET phase. The addition of both organophosphite and carbodiimide produces a blend which is stable with regard to the melting point and the heat of fusion of PET up to an extrusion temperature of 300°C. Incorporation of hindered phenol as a third stabiliser allows an extrusion temperature of 325°C. This temperature range is needed for blends which require higher processing temperatures and longer residence times in the extruder. The ternary blend of PAr/PC/PET shows consistency at temperatures ranging from 280°C to 325°C (see also Chapter 3).

2.2.2. *Non-organophosphite catalysts*

Sulphuric acid [42] and its salts have been mentioned as inhibitors for PET/PBT/PC blends. Suppression of transesterification in PC/PBT blends has also been achieved by the addition of about 1 wt% of nylon 6,6 or polyacrylamide [43]. In the case of bisphenol A polycarbonate (PC) and PET, the activity of a catalyst, either present as a residue from polymer synthesis, or purposely added before blending, may play an important role in controlling the chemical structure of the final product. Recently Fiorini *et al.* [44,45] have reported that catalysts based on lanthanide compounds possess a wide range of catalytic activity toward different reactions taking place during PET/PC reactive blending. The properties of the resultant product prepared by reactive blending of PET with PC can depend strongly on the reactions taking place during melt-blending. The selective activity of the catalyst toward exchange and degradation reactions and the solubility of the catalyst within the different phases may be key factors for the process. Hence, the choice of the appropriate catalyst becomes very important as it will allow materials with the desired properties to be prepared.

2.2.3. *Processing conditions*

In the case of immiscible mixtures, blending depends not only on the miscibility level of components, but also on the processing conditions. When mixing of components takes place in the molten state, the control of interchange reactions provides an opportunity to obtain alloys which are more homogeneous as compared to the corresponding physical mixture. Transesterification in polyester blends depends strongly on their initial compatibility and the blending conditions, such as temperature, residence time in the molten state, as well as percentage of each component.

During transesterification reactions a change in the melt viscosity is expected due to newly formed structures. This viscosity variation produces a corresponding change in the torque required to turn the Brabender mixer. Mondragon and Nazabal [34] have suggested a method of controlling interchange reactions of PC/PAr during processing in Brabender Plasticorder by plotting the torque variation against residence time. They also suggested an exchange reaction mechanism which analyses the viscosity variation as a function of time and blend composition at various temperatures.

During the transesterification of PC/PAr, the torque required to turn the Brabender *vs.* residence time was recorded. This torque is an indicator of melt viscosity. Torque variations of different PAr compositions *vs.* residence time at various temperatures are illustrated in Figure 3.

For all compositions the torque drops initially and becomes stable after some time when the two blend components are homogeneously mixed (Figure 3). The viscosity increases progressively with increase in residence time until it reaches a maximum value, which is attributed to exchange reactions between the two polymers. The torque increase is small because these transesterification reactions do not produce crosslinking. A decrease in viscosity at maximum torque shows that the degradation effect is stronger with re-

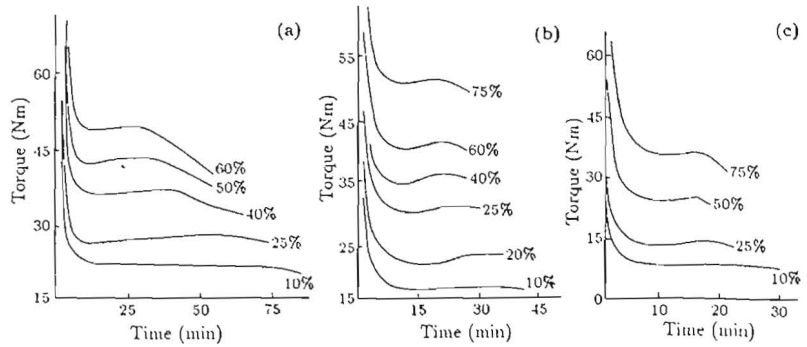

Figure 3. Torque variations of PAr compositions *vs.* residence time at: (a) 250°C; (b) 270°C; (c) 290°C [34]

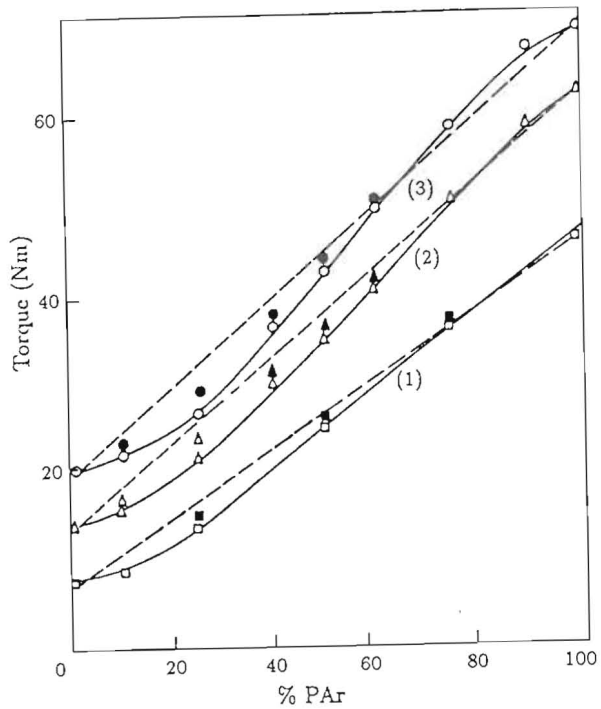

Figure 4. Torque data of blends before transesterification (empty symbols) and after transesterification (filled symbols) *vs.* mixture composition at the temperatures used: (1) 290°C; (2) 270°C; (3) 250°C [34]

spect to the exchange reactions. At 250°C (Figure 3a), the torque showed maximum at longer residence time. The torque increases with composition and the major variation occurs at about 25% PAr. Similar results are observed at higher processing temperatures, *i.e.*, 270°C and 290°C (Figure 3b,c). At higher temperatures maximum torque appears at shorter times. At these temperatures also major variation occurs at 25% PAr. At lower PAr content the maximum takes a longer time to appear and the torque change appears greater. This could be because of the higher viscosity of PAr, which necessitates the use of higher temperatures during processing when the PAr content increases. As a consequence, interchange reactions are faster when the blend has a high PAr content.

In Figure 4 it can be seen that at higher PAr contents the torque of the blend is closer to the torque of pure polymers. This observation could suggest that miscibility exists in PAr-rich compositions. However, the torque behaviour suggests that these polymers are immiscible or partially miscible and the first transesterification step develops in the PAr-rich phase. In

the absence of this transesterification reaction the torque data of the blend would have been below the torque data of pure polymers in all compositions. At low PAr content, the amount of copolymer which can be produced in the first step would be low, and hence it would have less influence on the torque data of the blend.

In Figures 3 and 4 it can be seen that the interchange reaction consists of two steps. The first step is fast and occurs in the PAr-rich phase, but it is not observable in the torque–time plot. The second step proceeds between the two phases of the blend and produces slope variation in the torque. As shown in Figure 3 at low PAr contents, the variation between the maximum and the stabilised torque is higher because of the smaller amount of PAr-rich phase.

During blend preparation in the Brabender it was observed that when the torque stabilised, the transparency of mixture varied with the temperature applied. Thus, at 250°C, blends with a PAr content of more than 60% were transparent, whereas at 270°C this limit decreased to 50% PAr, and at 290°C the same composition was observed to be transparent. Blends with a lower PAr content appeared opaque at these temperatures. These observations suggest that the miscibility limit in this blend exists between 50 and 60% PAr. Transparency can be due to copolymer formation in the PAr-rich phase, which could act as a compatibilising agent at high PAr contents. Moreover, at higher melt temperatures transesterification takes place more quickly and for this reason the higher the temperature, the lower the PAr content necessary for transparency to be observed.

In all compositions when the maximum in the torque–time curves was attained, transparency was observed in both melt and solid states. This is a clear indication of a structural change in the initially immiscible blends due to transesterification and it shows that the copolymers formed are fully amorphous. The above observation indicates that the exchange reaction between PC and PAr can be controlled by selecting an adequate temperature, thus allowing copolymer formation during a different residence time.

More recently, it has been observed that ester–carbonate interchange reactions occur even in the solid state at temperatures below 230°C [46]. Mixtures of oligomers derived from bisphenol A polycarbonate and polyesters (PET or poly(arylester)) were precrystallised and subjected to solid-state polymerisation in the temperature range 180–230°C. During this reaction both chain extension and interchange occurred. High molecular weight co-poly(ester–carbonate)s were obtained at the end of solid-state polymerisation. Analysis of polymer structure by a combination of techniques, such as selective dissolution, FTIR, and ^{1}H NMR, provide an evidence for the occurrence of carbonate–ester exchange reaction.

3. Methods of analysing transreactions in polymer blends

3.1. *IR spectroscopy*

Several methods have been used for analysing transreactions in polymer blends. One of the most commonly used techniques is infrared spectroscopy (IR), which originates from molecular vibrations that cause changes in the dipole moment and polarisability of molecular chains. These spectra are unique to each molecule and hence reflect the chain structure.

Transreactions in polycondensates lead to the formation of new copolymers. If we consider a system of PET and PC, new copolymers such as aromatic ester and aromatic carbonate will be formed due to transreactions. The progress of evolution of new components can be inferred by IR spectroscopy [47–50].

Specific vibration absorption bands of carbonyl groups in PET and PC are at 1720 and 1780 cm^{-1}, respectively. The stretching vibration of the carbonyl group in aromatic ester and aromatic aliphatic carbonate show specific absorption bands [47] at 1070, 1740, and 1770 cm^{-1}. When

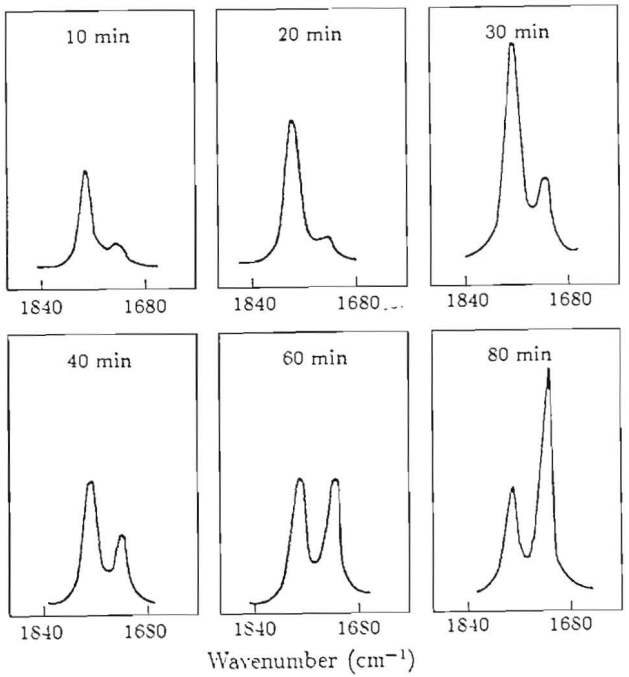

Figure 5. IR spectra of soluble fractions extracted with CH_2Cl_2 from a PET/PC blend (1:1 by wt) melt-mixed at 270°C for different periods of time [47]

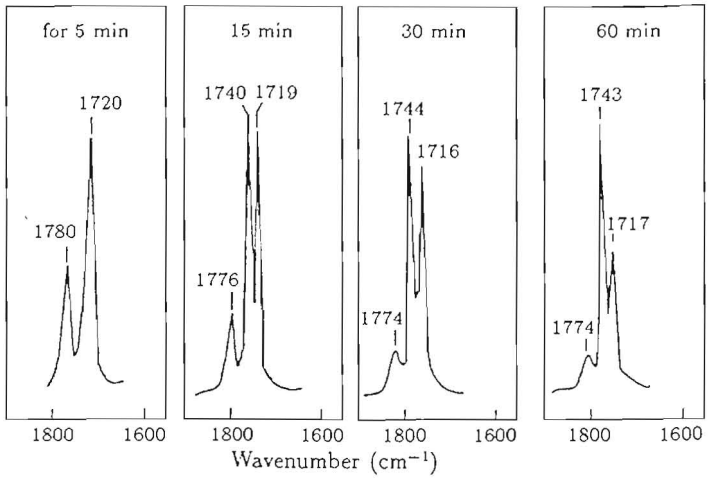

Figure 6. The spectra recorded for PET/PC blends (1:1 by wt) prepared at 300°C for: 5 min; 15 min; 30 min; 60 min [47]

PC/PET blends were melt-mixed for various periods of time and extracted with CH_2Cl_2, which is a good solvent for PC, significant changes occurred in the IR spectrum of the soluble fraction (Figure 5). For longer periods of mixing a progressive evolution of the band at 1720 cm^{-1} was observed. When the blending temperature was raised to 300°C, new absorption bands were seen at 1070 and 1740 cm^{-1}, and the band at 1780 cm^{-1} was shifted

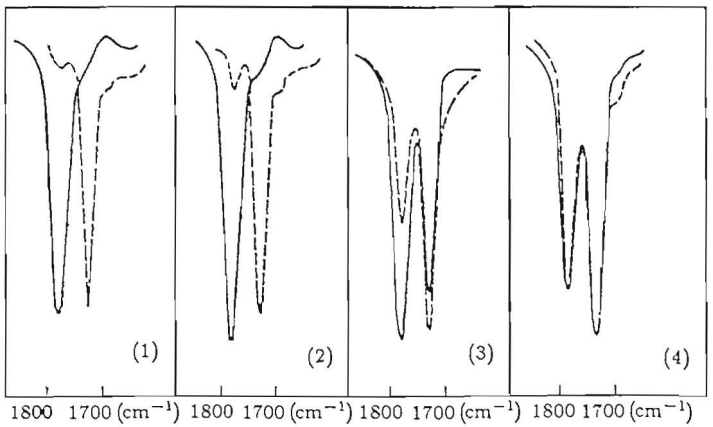

Figure 7. Evolution of C=O stretching bands in a PC/PBT blend (50/50 by wt) as a function of reaction time at 243.5°C: (1) 0 min; (2) 5 min; (3) 10 min; (4) 15 min; (—) soluble fraction; (----) insoluble fraction [47]

to 1770 cm^{-1}. The intensity of the bands at 1070 and 1740 cm^{-1} increased with mixing time (Figure 6). The occurrence of new bands and the band shift indicate formation of aromatic ester and aliphatic–aromatic carbonate by interchange reactions.

For a PC/PBT system similar observations were made [48]. The progressive appearance of absorptions at 1780 cm^{-1} and 1720 cm^{-1} in the soluble fraction indicates transesterification (Figure 7). At longer reaction times new bands appeared at 1740 cm^{-1} and 1070 cm^{-1} and the band at 1780 cm^{-1} shifted to 1770 cm^{-1}. As mentioned earlier, the bands at 1070 cm^{-1} and 1740 cm^{-1} are characteristic of an aromatic ester structure.

The band at 1070 cm^{-1} can be attributed to a complex vibration of the *para*-disubstituted phenyl to the right of the ester structure influenced by the neighbouring –COO group [48]. The absorption at 1770 cm^{-1} results from the –C=O stretching of a mixed aliphatic–aromatic carbonate.

In the case of ternary blends (PC/PAr/PET) the situation is more complex [40], since the aromatic ester groups, the presence of which is an indication of exchange reactions, exist in the system itself. Thus the changes in the infrared spectrum will be more subtle and some of the exchange products will not be distinguished from the reactants. Figure 8 shows the infrared spectra of the unstabilised blend as extruded, the unstabilised blend after isothermal treatment at 300°C for 30 min and the triply stabilised blend (details are given in Table 3). In curve 1 (Figure 9) there is evidence of an increase of the peak at 1070 cm^{-1}, but the corresponding changes in –C=O stretching region (1800–1700 cm^{-1}) are not clear. Curve

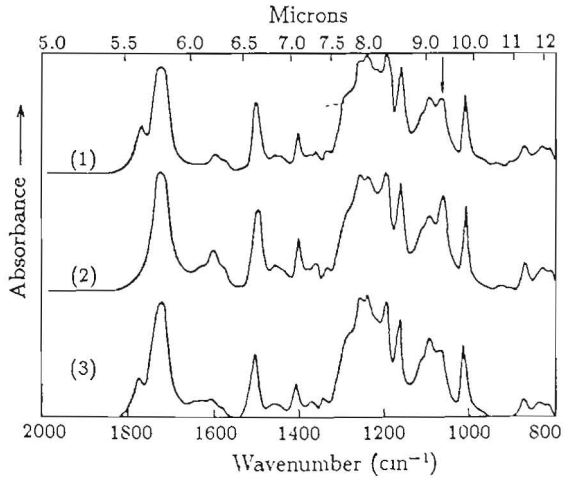

Figure 8. IR spectra of PAr/PC/PET blend without stabiliser and extruded at 280°C: (1) before isothermal test; (2) after 30 min at 300°C; (3) fully stabilised system (sample F, Table 3) [40]

Table 3. Results of isothermal DSC tests

Sample	Extrusion temp. (°C)	Stabilisers I[a]	II[a]	III[a]	Time at 300°C (min)	ΔH_f[c] (J/g)	T_m (°C)
A	280	x			0	12.2	249
					30	10.2	245.7
B	300	x			0	9.7	253.7
					30	6.2	247
C	300	x	x		0	12.2	249.7
					30	12.0	249.7
D	300	x	R-psty[b]		0	14.4	254
					30	10.0	251
E	325	x	x		0	7.7	251.8
					10	7.0	251.1
					30	5.3	244.4
F	325	x	x	x	0	11.8	252
					30	13.3	248
					60	10	246

[a] I Ultranox 624; II Stabaxol P-100; III Ethanox 330
[b] R-Psty, reactive polystyrene
[c] ΔH_f, Enthalpy of fusion

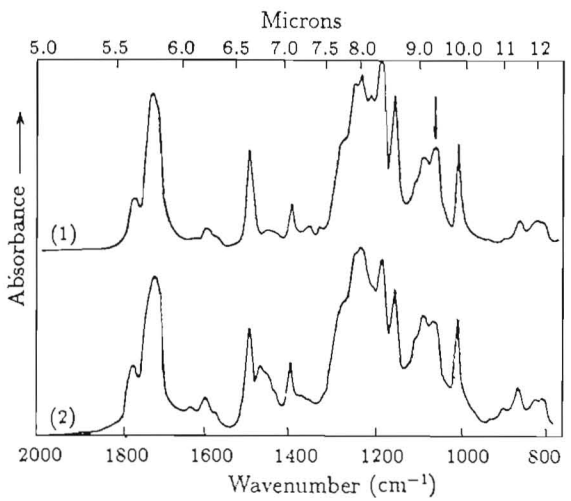

Figure 9. IR spectra of: (1) sample B (Table 3); (2) sample C (Table 3) after 30 min at 300°C [40]

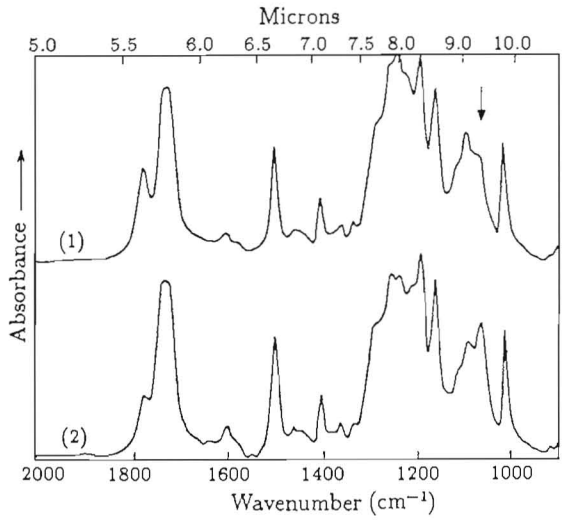

Figure 10. IR spectra of sample E (Table 3): (1) after 10 min at 300°C; (2) after 30 min at 300°C [40]

2 clearly shows a reduction of the bands at 1780 and 1770 cm^{-1} and increase in intensity for the bands at 1070 cm^{-1} and 1740 cm^{-1} indicating

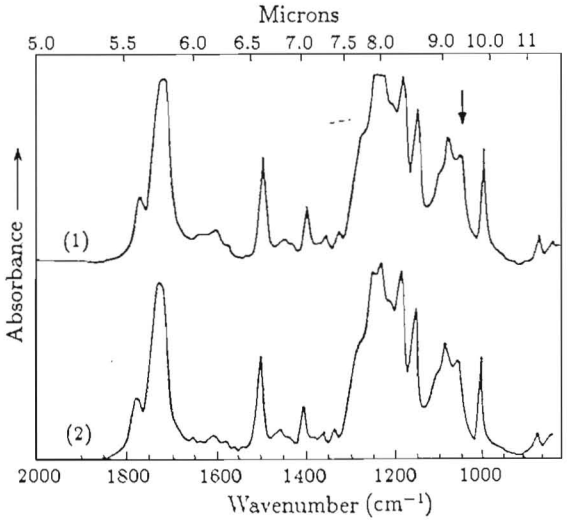

Figure 11. IR spectra of sample F (Table 3): (1) before isothermal test; (2) after 60 min at 300°C [40]

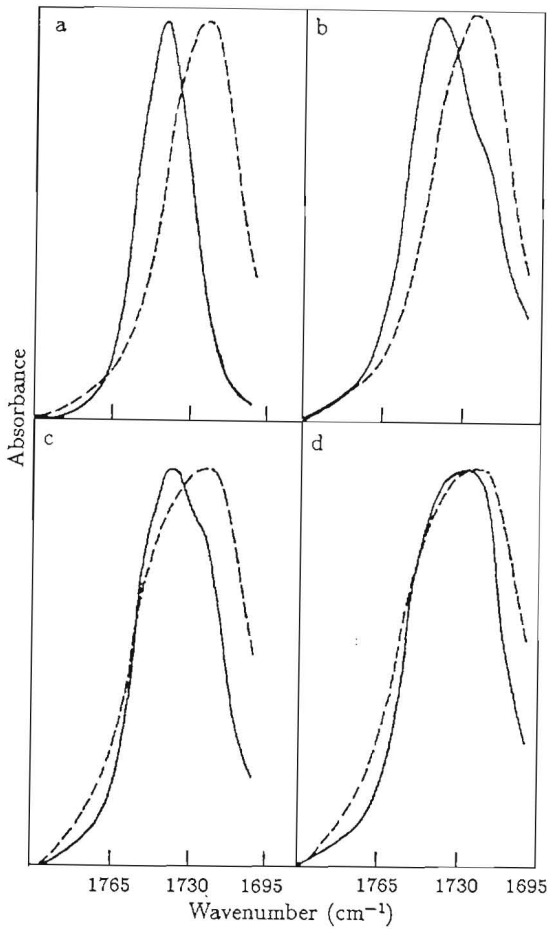

Figure 12. Evolution of C=O stretching bands after different treatment times: (a) 0 min; (b) 5 min; (c) 15 min; (d) 25 min (—); soluble fraction; (---) insoluble fraction [50]

formation of aromatic ester and loss of carbonate functionality. Figure 10 shows IR spectra of the blend after the addition of stabilisers I and II. The comparison of the curves proves the improved stability on addition of the stabiliser II. When the sample is heated at 300°C for 10 and 30 min, the absorption at 1070 cm^{-1} increases markedly (Figure 10). Figure 11 shows the spectrum of a fully stabilised system where, even after treatment at 300°C for 60 min, the absorption at 1070 cm^{-1} remains constant; an increase in absorption is expected whenever there is an exchange reaction.

Considering the PAr/PET system, –C=O stretching bands of pure PAr and PET appear at ~ 1740 and 1720 cm^{-1}, respectively [50], when no exchange reaction has taken place. When the 50:50 PAr/PET blend is heated at 300°C, transreactions occur and blocks of PAr appear in the insoluble fraction as well as PET sequences in the soluble fraction. When the reaction proceeds, the bands become similar, eventually leading to similar maximum and shape (Figure 12).

According to Berti *et al.* [51] the overlapping of several carbonyl stretching bands does not allow a clear separation of bands and conclusions based on IR data can be misleading. They postulate elimination of ethylene carbonate (EC) as a main reaction, rather than decarboxylation as was assumed by Godard *et al.* [32]. This was inferred by the presence of a small peak at 1810 cm^{-1} observed when melt-mixing of PC and PET was carried out in a closed system, which disappeared when the reaction was performed in an open system, under vacuum, or in a stream of nitrogen.

3.2. *NMR spectroscopy*

Valuable insights regarding transreactions occurring in polycondensates are provided by ^{1}H, ^{13}C, and ^{31}P nuclear magnetic spectroscopies.

3.2.1. *^{1}H and ^{13}C nuclear magnetic resonance spectroscopies*

For the PC/PBT system, important information can be obtained from the region between 8 and 8.4 ppm [48]. The NMR spectra in this region for PC/PBT (50/50 by wt) observed after different reaction times at 253°C (Figure 13) show progressive appearance of terephthalic ester units substituted by one or two aromatic groups. Significant changes occur in the region between 7 and 7.5 ppm corresponding to aromatic protons of bisphenol A

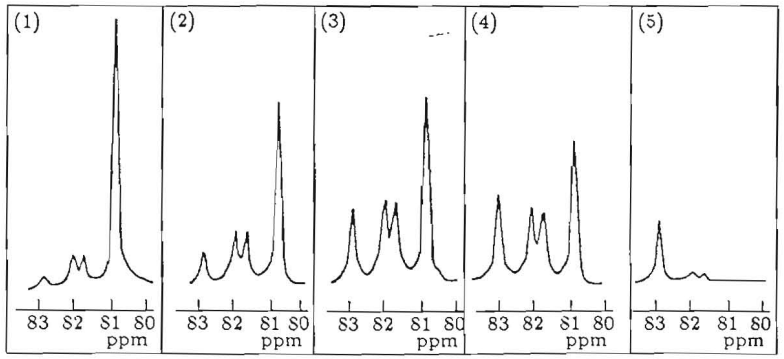

Figure 13. NMR peaks of protons of terephthalate units in the PC/PBT system (50/50 by wt) after different reaction times at 253°C, solvent $CDCl_3$: (1) 30 min; (2) 60 min; (3) 100 min; (4) 200 min; (5) bisphenol A polyterephthalate [48]

Table 4. Evolution of PBT ^{13}C peaks and relative intensities during the reaction (chemical shifts in ppm relative to TMS)

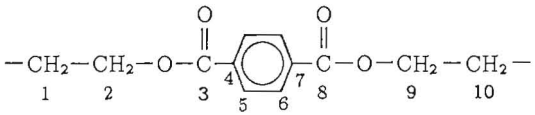

Attribution	$C_{1,10}$	$C_{2,9}$			$C_{3,8}$		$C_{4,7}$			$C_{5,6}$		Reaction time (min)
Chemical shifts (ppm)	23.8	65.7	68.1	68.7	168.3	167.5	132.3	132.9	133.4	128.9	129.6	
Relative intensities	43	30	NM	NM	31	NM	NM	30	NM	100	NM	15
	41	26	NM	5	29	3	3	27	3	86	15	31
	39	22	3	9	20	11	6	21	6	68	35	75
	35	19	4	8	21	14	5	22	5	60	41	100
	33	18	7	7	17	16	7	21	7	56	45	200

NM: not measurable

and the region around 4.2 ppm corresponding to a methylene group adjacent to oxygen ($-CH_2-O$) as a result of modifications in the surroundings due to interchange reactions.

^{13}C NMR spectra of PC/PBT mixtures during the reaction show that the relative intensities of the carbon signals corresponding to PBT carbons decrease progressively.

Table 5. Evolution of PC ^{13}C peaks and relative intensities during the reaction (chemical shifts in ppm relative to TMS)

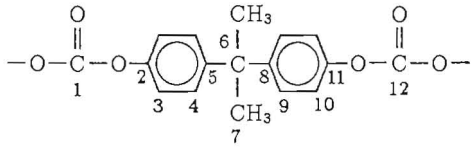

Attribution	$C'_{1,12}$			$C'_{2,11}$		$C'_{3,10}$		$C'_{4,9}$	$C'_{5,8}$	C'_6	C'_7	Reaction time (min)
Chemical shifts (ppm)	154.8	155.8	156.3	147.7	147.3	119.1	119.6	127.2	148.9	41.6	28.7	
Relative intensities	9	NM	NM	23	NM	75	NM	91	30	18	30	15
	6	4	NM	19	6	59	19	85	31	20	31	31
	2	6	NM	14	11	46	41	75	27	21	33	75
	NM	9	NM	15	18	36	47	74	30	20	34	100
	NM	6	4	12	21	34	46	67	28	17	30	200

NM: not measurable

The labelling of carbons is as shown below.

(C)

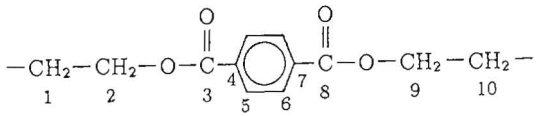

(C′)

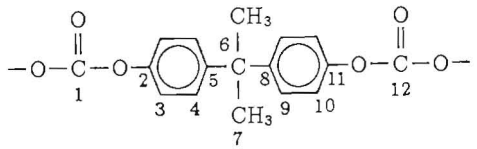

Tables 4 and 5 show changes in the relative intensities of PBT and PC ^{13}C peaks during reaction.

The new $C_{3,8}$ band appearing in the spectrum is due to the substitution of a butylene group by bisphenol A. The splitting of the $C_{4,7}$ peak at 132.9 ppm into two symmetrical absorptions at ±0.5 ppm from the initial band is also a result of the substitution. Considering C_5 and C_6 the peak at 129.6 ppm indicates asymmetrically substituted terephthalate groups while the peak at 128.9 ppm characterises the carbon atoms substituted either by two butylene groups or by two bisphenol A groups. The $C_{2,9}$ peak corresponding to the carbon of the $-CH_2-O$ groups of PBT is at 65.7 ppm. The two new bands at 68.1 and 68.7 ppm probably result from the appearance of aliphatic-aromatic carbonate and aliphatic-aliphatic carbonate units. The presence of three types of carbonate ester units ($C'_{1,12}$) is clear from peaks at 156.3 ppm, 155.8 ppm and 154.8 ppm corresponding to ester carbonate bearing two butylene groups, one butylene and one bisphenol A group and two bisphenol A groups respectively. The $C'_{2,11}$ and $C'_{3,10}$ signals of bisphenol A groups are split into two bands due to the simultaneous presence of bisphenol A carbonate and bisphenol A terephthalate units in the copolyester. The $C'_{5,8}$, C'_6, and C'_7 bands remain practically unchanged during the reaction.

Similar changes occur in the case of PC/PET systems (Tables 6 and 7) [32].

(C)

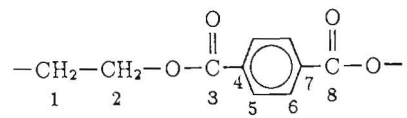

(C′)

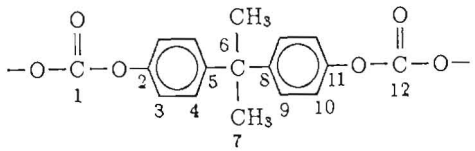

Table 6. Evolution of PET ^{13}C peaks and relative intensities during the reaction (chemical shifts in ppm relative to TMS)

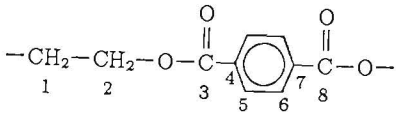

Attribution	$C_{1,2}$					$C_{3,8}$		$C_{4,7}$		$C_{5,6}$		Reaction time (min)
Chemical shifts (ppm)	66.7	65.7	65.5	63.7	62.9	165.3	164.2	133.3	133.6	130	129.6	
Relative intensities	NM	NM	NM	NM	9	8	NM	5	8	21	41	10
	NM	5	NM	4	8	5	3	9	8	26	30	20
	3	5	3	5	4	4	5	12	4	43	26	40
	3	8	7	5	NM	6	9	16	5	62	30	80
	6	10	7	6	NM	5	8	17	5	60	24	100

Reaction at 235°C. NM: not measurable

The relative intensities of the "carbon" signals (165.3, 133.6, 129.6 ppm — $C_{3,8}$, $C_{4,7}$, $C_{5,6}$) corresponding to PET carbons decrease progressively. The new peaks appearing at 164.2, 133.8 and 130.0 ppm can be attributed to terephthalate units substituted by an aromatic species. The peak corresponding to methylene carbons ($C_{1,2}$) undergoes a more complex evolution. The peak at 62.9 ppm decreases gradually, finally giving rise to two peaks at 65.7 and 63.7 ppm. This indicates progressive substitution of a

Table 7. Evolution of PC ^{13}C peaks and relative intensities during the reaction (chemical shifts in ppm relative to TMS)

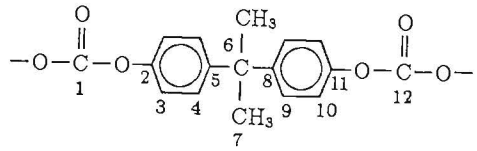

Attribution	$C'_{2,11}$			$C'_{3,10}$		$C'_{4,9}$	$C'_{5,8}$		C'_6		C'_7	Reaction time (min)
Chemical shifts (ppm)	156.3	148.9	148.6	120.8	120.2	114.1	127.8	148.0	143.1	42.4	42.0	30.8	
Relative intensities	NM	19	8	21	86	3	114	24	NM	12	NM	42	102
	NM	20	10	35	77	11	123	19	NM	18	5	49	20
	NM	11	18	47	59	19	125	18	NM	15	6	55	30
	5	12	22	64	53	31	150	22	6	16	10	63	80
	6	12	21	59	43	28	128	18	5	17	11	60	100

Reaction at 235.5°C, catalyst: 0.2% by wt of tetrabutyl orthotitanate. NM: not measurable

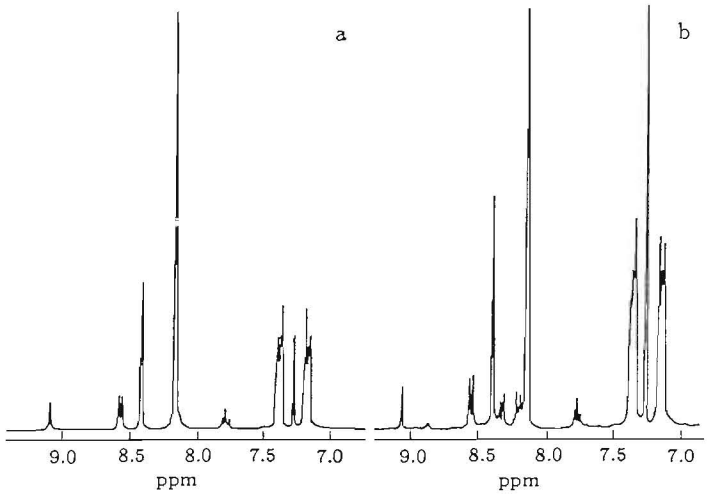

Figure 14. ^1H NMR spectra of (a) PAr/PBT blend before transesterification; (b) soluble fraction of PAr/PBT after transesterification [52]

neighbouring terephthalate by a carbonate group, which gives rise to two non-equivalent methylenes. At longer reaction times another set of two peaks appears at 66.7 and 65.7 ppm, indicating some reactions consecutive to the transesterification. A carbon dioxide elimination from the aromatic–aliphatic carbonate group with ether formation was suggested. Considering the peaks of PC groups (Table 7), $C'_{2,11}$ and $C'_{3,10}$ peaks occurring in PC at 148.9 and 120.2 ppm are initially split, two new peaks appear at 148.6 and 120.8 ppm belonging to new bisphenol A-terephthalate groups.

A comparison of ^1H NMR spectra of a PAr/PBT blend before and after transesterification (Figure 14) proves new signals at 8.3 and 8.21 ppm between those of terephthalate protons (a) and (b) (Figure 15) ($\delta_a = 8.41$, $\delta_b = 8.16$) which can be attributed to the aromatic protons of the asymmetrically substituted terephthalate unit, indicating transesterification [52]. The absorptions corresponding to aromatic protons of the symmetrically substituted isophthalic units (d) appear at 9.08, 8.56 and 7.78 ppm as a singlet, a doublet, and a triplet, respectively. These units can react with the PBT units giving rise to a type (e) structure. The absorptions at 8.87 (singlet), 8.48 (doublet) and 7.71 (triplet) ppm can be attributed to the aromatic protons of the asymmetric isophthalate units.

Thus the occurrence of transreactions which drive the chemical structure toward that of a random copolymer is clearly indicated by the modification of all the regions of the NMR spectrum. From ^1H NMR there is also evidence of the formation of ethylene carbonate and the occurrence of side reactions [51]. In a PC/PET blend it is observed that the molar ratio

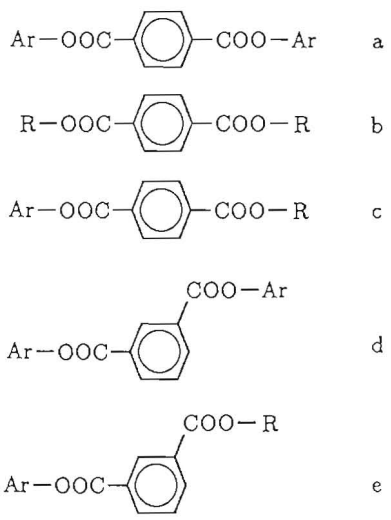

Figure 15. Structures referred to in the text [52]

of ethylene glycol protons to the terephthalate protons changes from 1 to 0.84 while the molar ratio of bisphenol A to terephthalate units does not change. The observed change in molar ratio is assumed to be due to the elimination of EC from the reaction medium. In fact a small sharp peak at $\delta = 4.51$, typical of EC, is observed when the samples are prepared by melt-mixing in a closed system, but it disappears in the spectra of samples prepared under reduced pressure [51].

Thus ^{1}H and ^{13}C NMR spectroscopies prove to be useful techniques to follow transreactions taking place in polycondensates during melt-mixing (see also Chapter 1).

3.2.2. ^{31}P *nuclear magnetic resonance spectroscopy*

Phosphorus-31 magic-angle spinning (MAS) NMR is useful in tracking the chemistry of phosphites in polymer blends, since it can determine, through the chemical shift interaction, the identity of phosphorus species present in the solid state and, to high precision, the relative and absolute concentrations of these moieties.

The efficiency of the technique can be exemplified by the studies on the behaviour of Ultranox 624, bis(2,4-di-t-butylphenyl pentaerythritol) diphosphite (BTBP), an organophosphite stabiliser in a blend of PC, PET, and PAr prepared at 280°C [53]. Three concentrates of Ultranox 624 in polycarbonate were prepared under different conditions in a twin screw extruder (Table 8). The ^{31}P CPMAS (cross-polarisation magic-angle spinning) spectrum of neat BTBP shows an isotropic chemical shift line for BTBP at 115.5 ppm (Figure 16), which was confirmed by the use of side band suppression pulse sequences. The broad peak centered at ~ 7 ppm is identified as an amorphous orthophosphite or phosphonate. It is reported that organophosphites can undergo oxidation to an organophosphate es-

Table 8. Summary of concentrate preparation in twin screw extruder

BTBP concentrate	Polycarbonate (Dow's caliber)	Drying conditions	Compounding atmosphere
A	300–15 (low MW)	Mild	Air
B	300–15 (low MW)	Rigorous	N_2 blanket
C	300–3 (high MW)	Rigorous	N_2 blanket

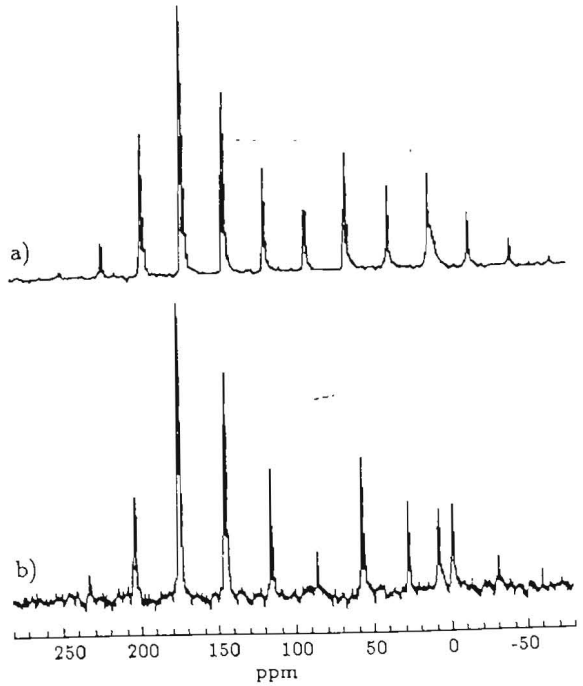

Figure 16. Phosphorus-31 CPMAS spectra of neat BTBP (26% by wt in a non-phosphorus containing organic binder): (a) 3200 kHz, 100 acquisitions, arrows indicate isotropic chemical shifts; (b) 3500 kHz, 10 acquisitions. Both spectra represent 256 acquisitions at 120.5 MHz using a 2 ms contact pulse and 10 s recycle time [53]

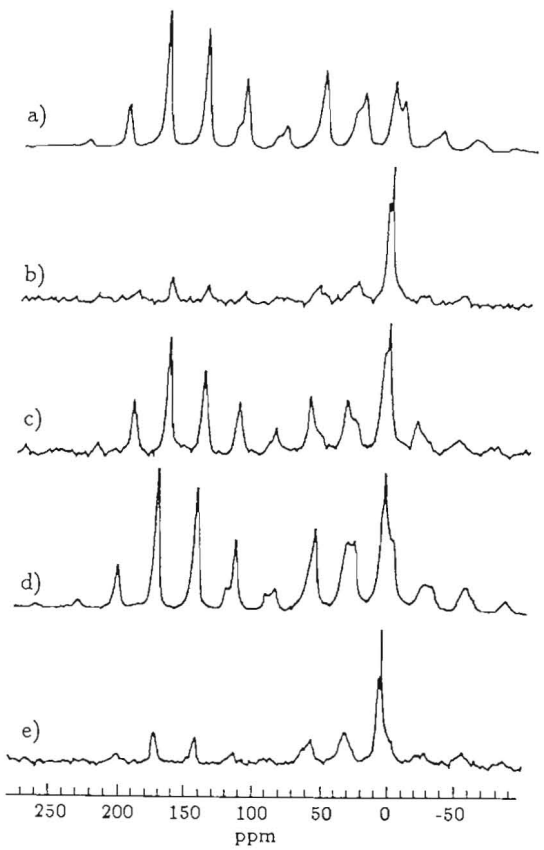

Figure 17. Phosphorus-31 CPMAS spectra of the PC/BTBP concentrate A (Table 8): (a) as extruded, 3500 kHz, 14 000 acquisitions; (b) after drying in air-circulating oven, 16 h at 100°C, 3200 kHz; (c) after drying under vacuum without heating, 3200 kHz; (d) clear pellets of concentrate A, 3500 kHz; (e) cloudy pellets of concentrate A, 3500 kHz. All spectra represent 256 acquisitions at 120.5 MHz using a 2 ms contact pulse and 10 s recycle time [53]

ter or hydrolysis to an organophosphonate and isotropic chemical shifts of these species should be ±10 ppm to that of 85% phosphoric acid at 0 ppm.

Solid-state ^{31}P NMR of concentrates. There is an overall increase in the line width in the spectra of PC/BTBP concentrates relative to that of the neat BTBP which can be due to the loss of crystallinity induced by the compounding process (Figure 17). Comparing the spectrum of the concentrate after heating in an air oven at 100°C for 16 h and that after

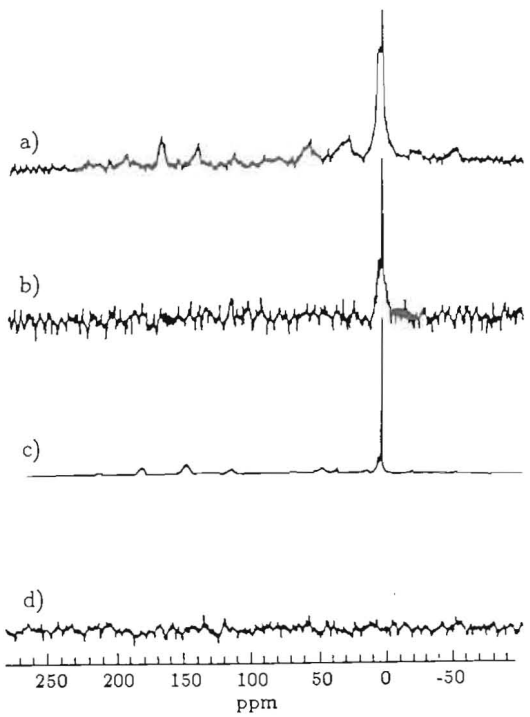

Figure 18. Phosphorus-31 NMR spectra of the PC/BTBP concentrate A: (a) CPMAS spectrum of concentrate A dried in an air-circulating oven at 100°C (as in Figure 17b); (b) TOSS FID of the concentrate dried in an oven at 100°C; (c) CPMAS spectrum of pulverised concentrate A stored in ambient conditions for 30 days; (d) CPMAS spectrum of neat polycarbonate [53]

vacuum drying, the former shows higher intensity of the resonance near 7 ppm. Following heating under air, a fraction of the pellets turned cloudy; their spectrum showed predominance of two impurity peaks at 5.9 and 8.3 ppm, apart from that at 7 ppm (Figure 17).

If we compare the CPMAS of the concentrate with total suppression of spinning side bands (TOSS; when TOSS is employed following the use of single 90° pulse for the creation of transverse magnetisation, the technique is called TOSS FID), it is seen that the signal for phosphorus (115.5 ppm) is not visible, indicating that the species is in an immobile environment (Figure 18). But the peak at 7 ppm is seen in TOSS FID, also indicating that the species is in a mobile or relaxed environment (Figure 18). TOSS FID confirms the presence of other impurity peaks. When the unheated pulverised sample was exposed to air for 30 days, a similar change occurred when heated under air. Thus the new products must have formed by either

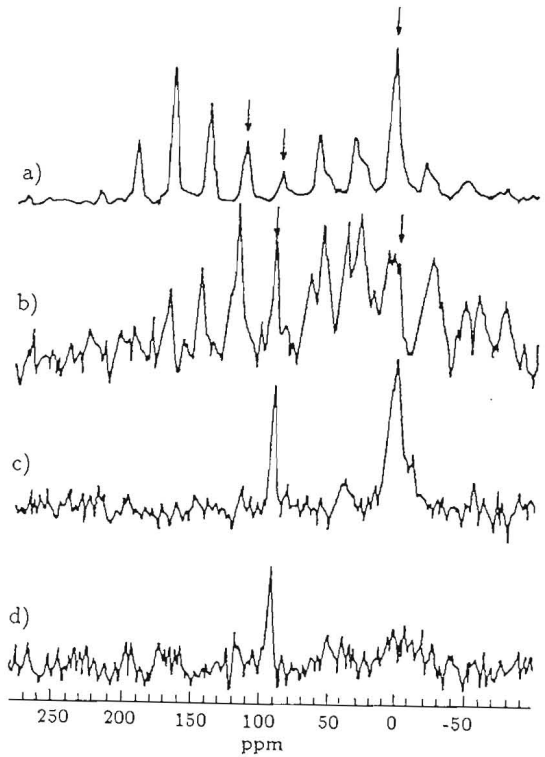

Figure 19. Phosphorus-31 spectra of blends prepared from PC/BTBP concentrate A (Table 8), 3200 kHz: (a) CPMAS spectrum of the PC/BTBP concentrate after drying under vacuum for 16 h in an air-circulating oven; (b) CPMAS spectrum of a polymer blend prepared using the PC/BTBP concentrate; (c) TOSS spectrum of the same blend, 3600 acquisitions, 2 s recycle delay; (d) TOSS PPS spectrum using a 40 μs delay of the same blend, 12 000 acquisitions [53]

oxidation or hydrolysis.

Solid-state ^{31}P NMR of polymer blends. The CPMAS NMR spectrum of the actual PC/BTPB concentrate used to produce the polymer blend (acquired at a high signal/noise (S/N) ratio) shows an impurity peak at 95 ppm also (Figure 19). The ^{31}P MAS NMR spectrum of the ternary blend shows complete absence of a peak at 115.5 ppm (Figure 19). This was confirmed by TOSS and TOSS PPS (TOSS protonated phosphorus suppression) spectra. The former shows resonances at 95 and 7 ppm as well as an extra signal at 42 ppm which could be an additional product of the chemistry of BTPB. The TOSS PPS spectrum for a delay time of 40 μs

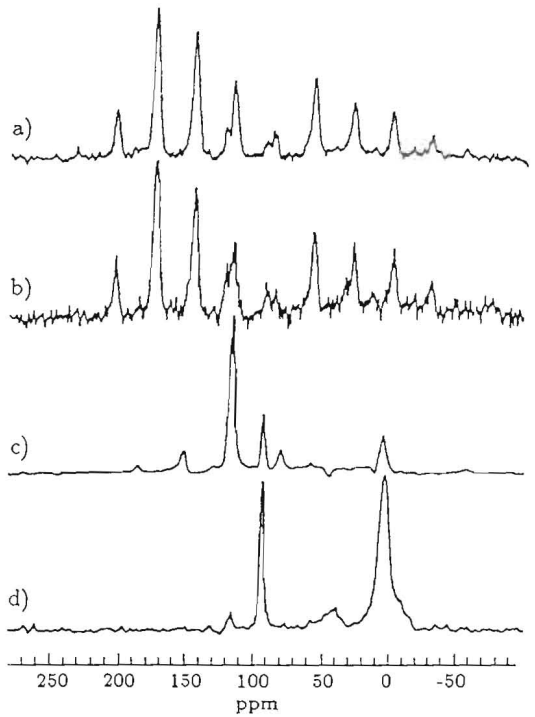

Figure 20. (a) CPMAS spectrum of PC/BTBP concentrate C (Table 8); (b) the corresponding polymer blend; (c) TOSS spectrum of concentrate B (Table 8); (d) the corresponding polymer blend [53]

shows the absence of a peak at 7 ppm and a reduction in the intensity of the peak at 95 ppm.

The absence of the peak in the TOSS PPS spectrum indicates a protonated phosphorus species in a relatively rigid environment, unlike the species in the original concentrate. Thus the 7 ppm species in the blend cannot be a phosphate, but a phosphonate resulting from the hydrolysis of the phosphite triester. For such a species, which has a proton directly bonded to the phosphorus, we can expect short TOSS PPS delays to produce complete loss of intensity.

The results of DSC analyses show that whenever the phosphite is converted into phosphonate, the melting point and the heat of fusion of PET are stabilised and transreactions are suppressed [54].

From the above discussion it is clear that ^{31}P NMR spectroscopy provides information on the actual mechanism by which phosphitic stabilisers suppress transreactions in blends of polycondensates.

3.3. *Differential scanning calorimetry*

DSC has been reported to be an effective qualitative technique to assess the extent of transreactions occurring in blends of polycondensates. Associated with transesterification, there will be a decrease in ΔH_f [55]. At advanced stages of transesterification, the crystallisable moiety will lose its ability to crystallise. If we consider blends whose components are noncrystallisable, such as bisphenol A polycarbonate and polyarylate, the T_g values of each component will move towards each other with progressive transreactions, eventually giving rise to a single T_g corresponding to the copolymer formed due to transesterification [40,47,55].

The copolymer produced by transreaction can enhance the miscibility of a system [47]. Multiple T_g values for a polymer blend indicate multiple phases. In the case of a PC/PET blend, the higher T_g corresponds to PC while the lower T_g corresponds to PET. Figure 21 shows the change in T_g with PET/PC blend composition. The higher T_g, related to PC, decreases at low levels of PET, then increases a little when the concentration of PET exceeds 60 wt %. The lower T_g, related to PET, increases with increasing PC content through a flat peak and then decreases.

The DSC thermograms (Figure 22) of PET/PC blended at different temperatures for 10 min show dual transitions when blending temperatures are below 300°C. A single transition is found for the sample blended at 300°C. Figure 23 shows the change in T_g of the blends for various blending times at 270°C. It can be seen that, on prolonged mixing, the difference between the two transition temperatures decreases and they finally merge into one T_g, indicating the progress of transreaction.

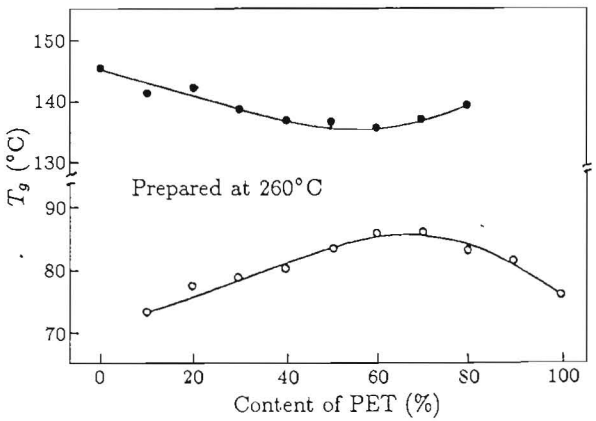

Figure 21. Change in T_g with PET/PC blend composition. Samples were annealed at 180°C for 60 min prior to the second run. Measurements were carried out by DSC at a heating rate of 40°C/min [46]

In the case of blends with a crystallisable moiety, such as PET with PAr and with PC, the transesterified polymers are noncrystallisable and exhibit a single T_g between that of the starting polymers [31,56]. If we consider blends of PBT with PAr and with PC, blends without transesterification show a single T_g, indicating amorphous miscibility of PBT and PAr, but without melting point depression, implying that PBT crystallises with exclusion of PAr. However, transesterified systems show higher T_g values than the corresponding physical blends and exhibit a marked melting point depression and a lower PBT crystallinity [57,58].

The physical blends of PC and PAr are found to exhibit two amorphous phases, a pure PC phase and a PAr-rich mixed phase [35], giving two separate T_g values at 149°C and 178°C, respectively. On controlled thermal treatment, transreaction between PC and PAr takes place leading to a new copolymer with a single T_g, depending on the original binary composition. The progress of reaction from block copolymers to random

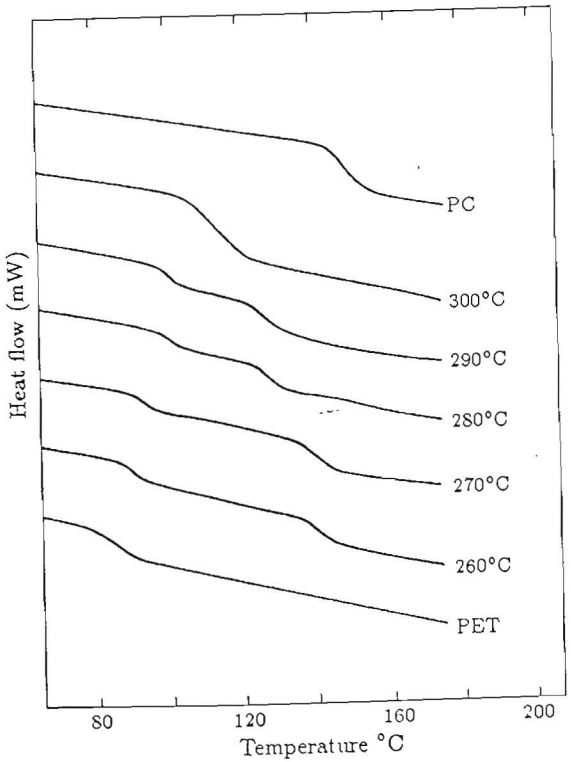

Figure 22. Change in DSC T_g behaviour of PET/PC (1:1 by wt) blended at different temperatures for 10 min [47]

copolymers can be traced by DSC [35]. The DSC curve of a PC/PAr blend (50/50) processed in a single screw extruder at 305°C (Figure 24) shows a single T_g corresponding to PC (a PAr-rich phase may also exist). But the blend extruded at 325°C shows a single T_g at 160°C, indicating complete miscibility (Figure 24). The DSC curves of PC/PAr blend film cast from methylene chloride solution reveal two T_g values but both transitions seem to have shifted toward each other, indicating partial miscibility (Figure 25). An interesting observation is that the extrudate at 285°C, which shows two distinct T_g values, exhibits a single T_g when injection moulded at a melt temperature of 290°C (Figure 26) and the originally opaque sample becomes transparent. The same sample when annealed at 180°C turns opaque. A solution-cast film of moulded sample was also prepared, the DSC thermograms of which show reappearance of T_g at 149°C (PC-rich

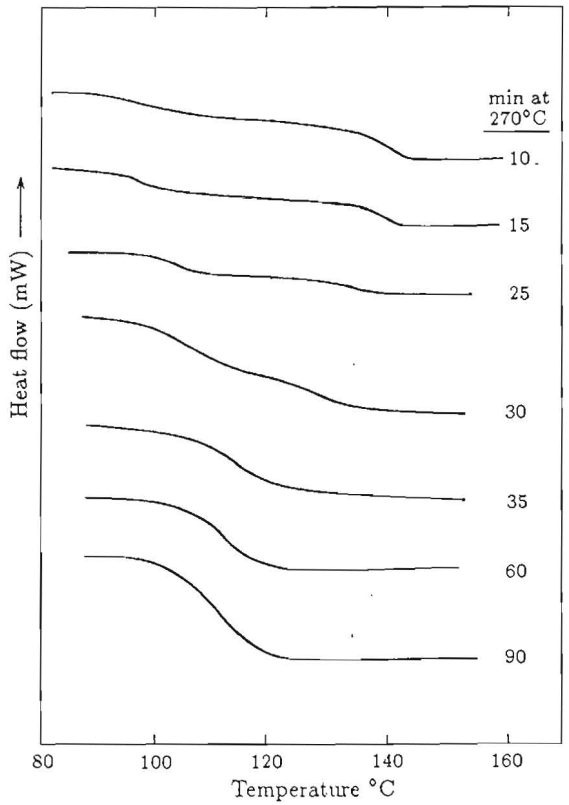

Figure 23. Change in DSC T_g behaviour of PET/PC (1:1 by wt) with blending time at 270°C [47]

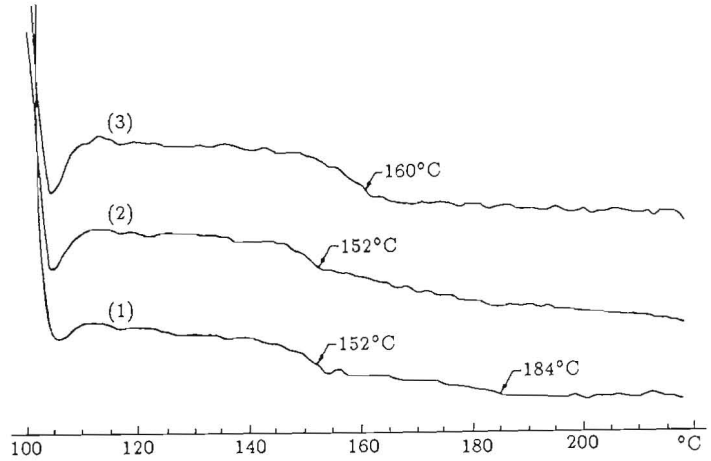

Figure 24. DSC curves of a PC/PAr blend (50/50) single screw extruded at: (1) 285°C; (2) 305°C; (3) 325°C [35]

phase), indicating phase separation. However, a solution-cast film of the blend compounded in a twin screw extruder shows a single T_g, confirming transesterification in advanced stages (Figure 25).

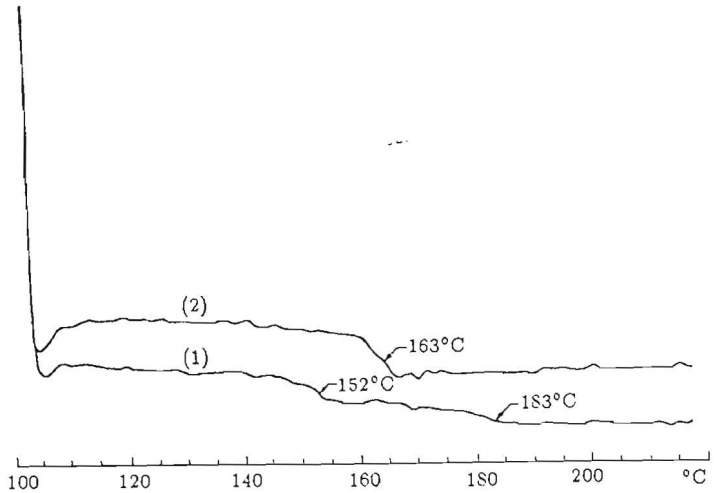

Figure 25. DSC curves of 50/50 PC/PAr blends: (1) resins dissolved in methylene chloride at 23°C and cast into a film; (2) twin screw extrudate dissolved in methylene chloride and cast into a film [35]

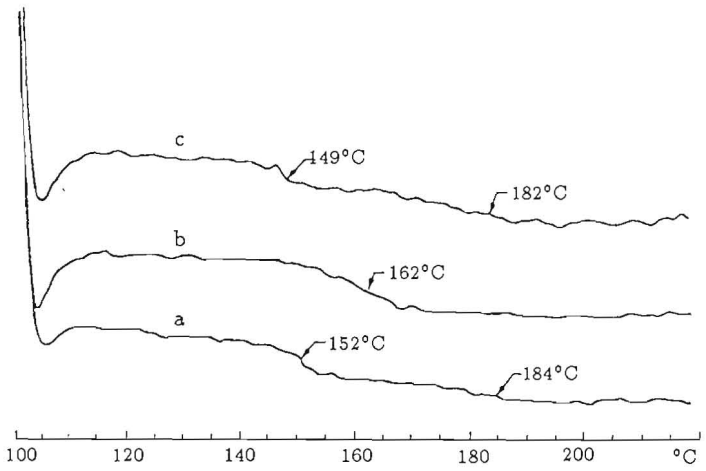

Figure 26. DSC curves of PC/PAr blends (50/50): (a) reproduction of curve (1) of Figure 25; (b) injection-moulded A; (c) sample of B dissolved in methylene chloride and cast into a film [35]

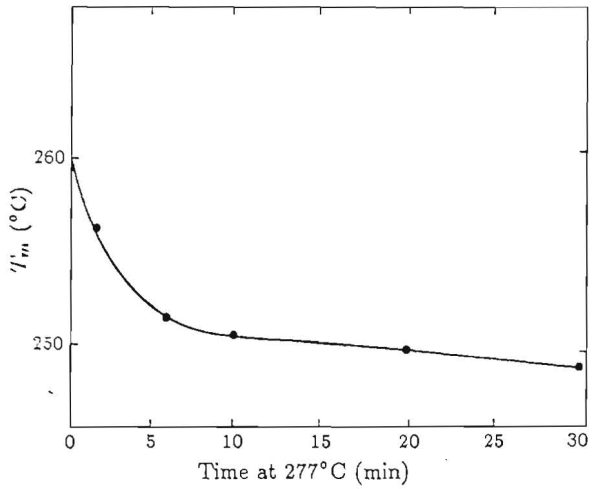

Figure 27. Change in melting point of copolyester in 50% blend (without additives) with time in the melt [38]

From the above discussion it is clear that DSC can be used as an efficient technique to follow transreactions. There are many reports of the use of DSC in studies regarding the inhibition of transesterification

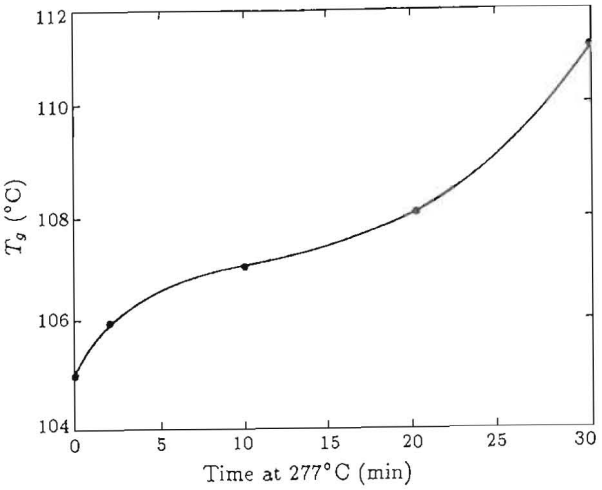

Figure 28. Change in T_g of 50% blend (without additives) with time in the melt [38]

[31,38,40,54,55,59]. A blend of polycarbonate and the copolyester based on 1,4-cyclohexane dimethanol and a mixture of terephthalic and isophthalic acids is known to undergo transesterification [38]. Figures 27 and 28 show

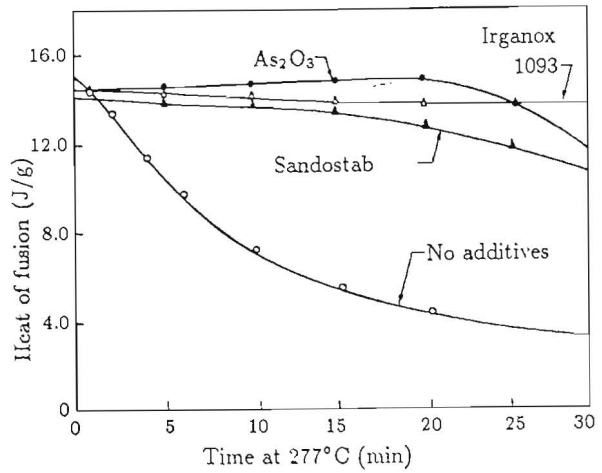

Figure 29. Effect of various additives on the crystallisability of copolyester from 50% blend held in the melt for various times [38]

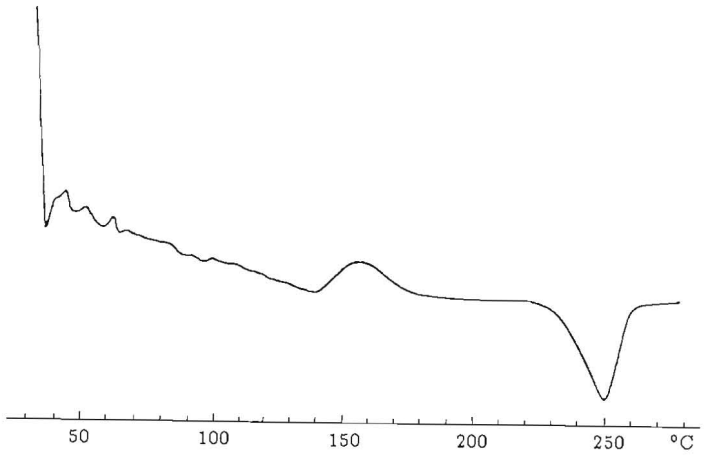

Figure 30. DSC scan of PAr/PC/PET ternary blend with concentrate A (Table 9), predried at 100°C for 16 h, after being held isothermally for 30 min at 300°C [54]

the change in T_m and T_g with time in the melt for the 50% blend containing only the residual catalyst from the copolyester. In order to inhibit the transesterification, arsenic compounds, or commercially available stabilisers were incorporated into the blends in a subsequent extrusion step. The

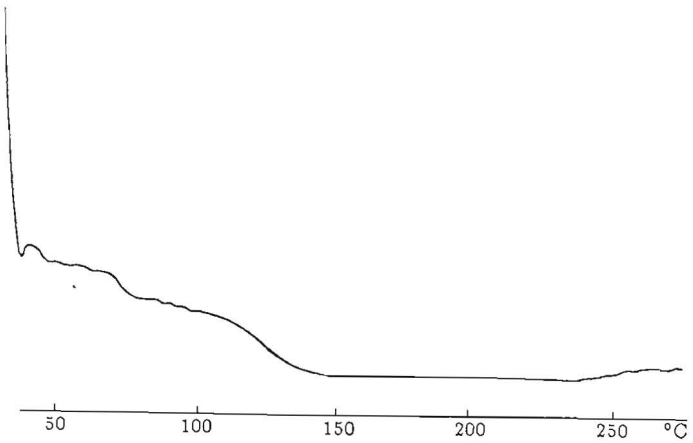

Figure 31. DSC scan of PAr/PC/PET ternary blend with concentrate A (Table 9), predried in vacuum at ambient temperature for 16 h, after being held isothermally for 30 min at 300°C [54]

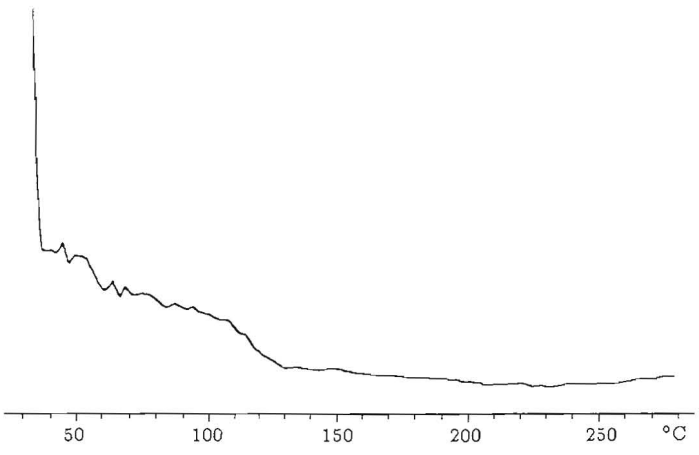

Figure 32. DSC scan of PAr/PC/PET ternary blend with concentrate B (Table 9), predried at 100°C for 16 h, after being held isothermally for 30 min at 300°C [54]

ability of As_2O_3 as well as phosphite stabilisers to preserve the crystallinity is evident from the heat of fusion values obtained by DSC (Figure 29).

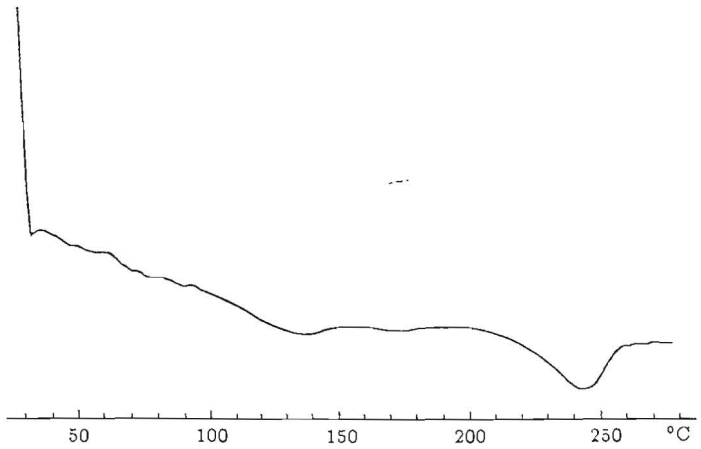

Figure 33. DSC scan of PAr/PC/PET ternary blend with concentrate C (Table 9), predried at 100°C for 16 h, after being held isothermally for 30 min at 300°C [54]

Cheung *et al.* reported the use of DSC to evaluate the effectiveness of stabilisers to inhibit transesterification in a ternary blend of PAr, PC and

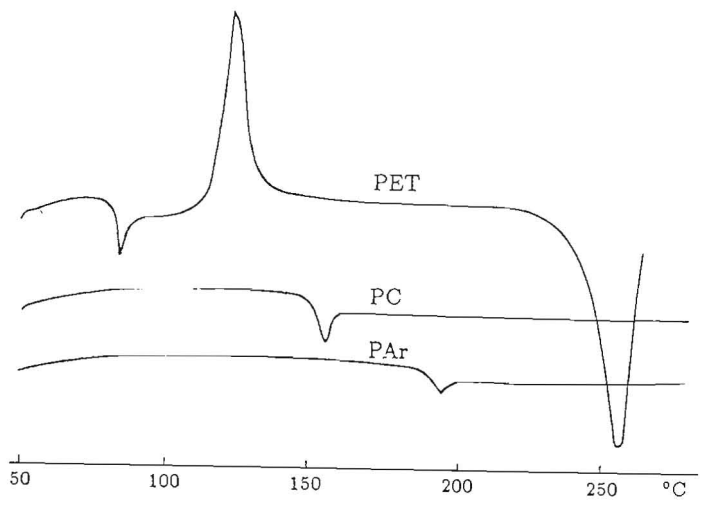

Figure 34. DSC thermograms of PET, PC, and PAr [40]

PET (50/20/30) [54]. The criterion is based on the retention of the melting point and the heat of fusion of PET [31,40,58].

Figures 30, 31, 32, and 33 show DSC thermograms of ternary blends stabilised with transesterification inhibitors, namely, Ultranox 624 and

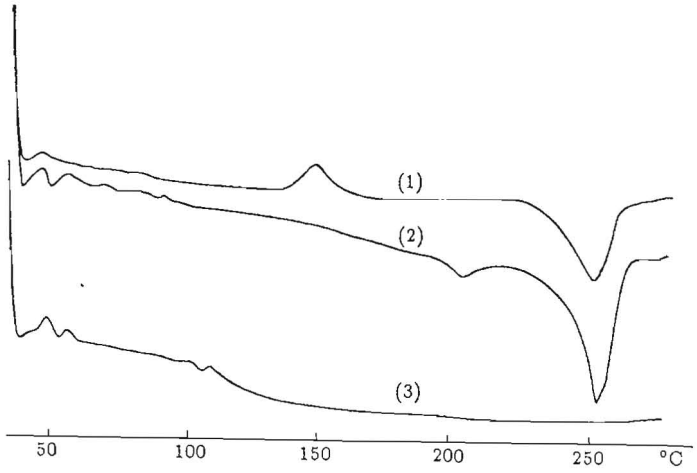

Figure 35. DSC thermograms of PAr/PC/PET (50/20/30) blend without stabiliser: (1) second step after extrusion at 280°C; (2) after annealing at 190°C for 1 h; (3) after 10 min at 280°C [40]

Table 9. Summary of concentrate preparation in twin screw extruder

Concentrate	Type of polymer	Drying conditions	Compounding atmosphere
A	PC	4 h, 100°C	Air
B	PC	18 h, 130°C	N_2 blanket
C	PET	18 h, 130°C	N_2 blanket

Stabaxol P-100. The stabilisers were incorporated into the blend by first preparing concentrates. The conditions of drying the resins for preparing the concentrates are summarised in Table 9. The stabilisers used were 0.5% by wt of Ultranox 624 and 0.25% by wt of Stabaxol P-100. Figure 30 shows the behaviour of the blend with concentrate A (predried at 100°C for 16 h) after being held isothermally at 300°C for 30 min. The retention of melting point of PET is clear from the melting endotherm. Figure 33 (blend with concentrate C (predried at 100° C for 16 h)) also shows the crystallinity of the blend. Figures 30 and 31 do not show melting endotherm indicating the occurrence of transesterification. ^{31}P NMR shows that concentrate A (as used to prepare the blend shown in Figure 30) and concentrate C (used to prepare the blend shown in Figure 33) contain phosphonate groups, and that concentrate A (used to prepare blend in Figure 31) and concentrate B (used to prepare blend in Figure 32) do not contain phosphonate species which can effectively complex with the residual catalyst present in PET

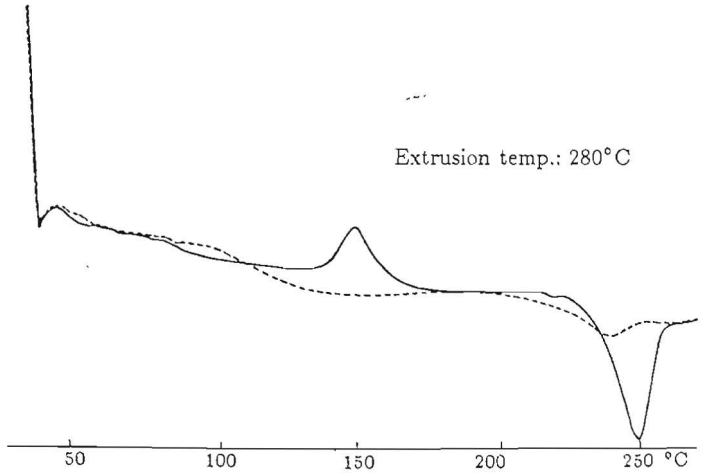

Figure 36. DSC thermograms of PAr/PC/PET without stabiliser: second scan (—); eighth scan (---) [40]

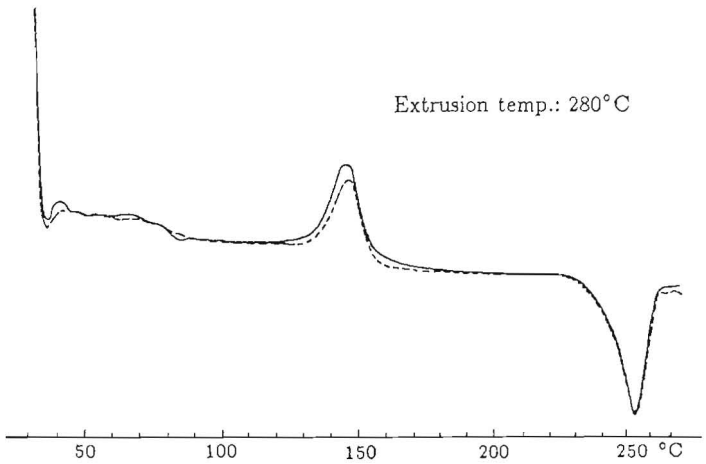

Figure 37. DSC thermograms of PAr/PC/PET with Ultranox 624: (—) second scan; (---) eighth scan (sample A, Table 3) [40]

leading to the inhibition of transesterification.

The effectiveness of a stabiliser system consisting of phosphites, polycarbodiimide, and hindered phenols which successfully inhibits transesterification at temperatures up to 325°C in a ternary blend of PET, PC, and PAr has been examined by thermal cycling using DSC [40]. Figures 34 and 35 show the DSC thermograms of PET, PC, and PAr and PAr/PC/PET (50/20/30) blend without stabiliser. The thermogram of the blend immediately after extrusion at 280°C clearly shows PET features (a glass transition temperature at 83°C, a cold crystallisation exotherm at 145°C, and a melting endotherm at 250°C). The glass transition temperatures of PAr and PC are not seen clearly because of PET's cold crystallisation exotherm. Curve (2) of Figure 35 shows a shift in glass transition temperatures of PC and PAr (150°C and 180°C instead of 145°C and 190°C) and gives evidence of the occurrence of transesterification to some extent. The third curve, which corresponds to the thermogram after annealing at 280°C, reveals a single T_g at 125°C and proves complete transesterification. When phosphite (Ultranox 624) was incorporated, the blend was fairly stable (extrusion temperature 280°C, annealed at 300°C for 30 min; T_m decreased by 3°C and ΔH_f by 2 J/g). However, when the extrusion temperature was raised to 300°C, a larger decrease in ΔH_f and T_m was observed. A combination of Ultranox and Stabaxol P-100 (polycarbodiimide) stabilises the blend at

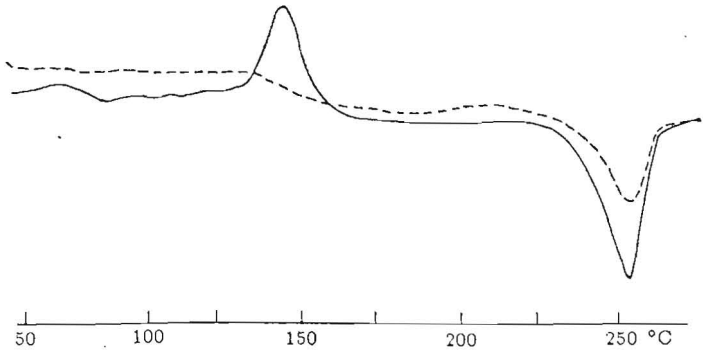

Figure 38. DSC second scan thermograms of PAr/PC/PET with Ultranox 624 extruded at 280°C (—) and at 300°C (---) [40]

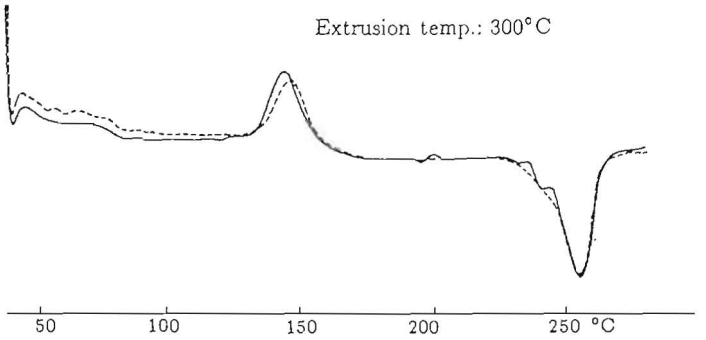

Figure 39. DSC thermograms of PAr/PC/PET with Ultranox 624 and Stabaxol P-100: (—) second scan; (---) eighth scan (sample C, Table 3) [40]

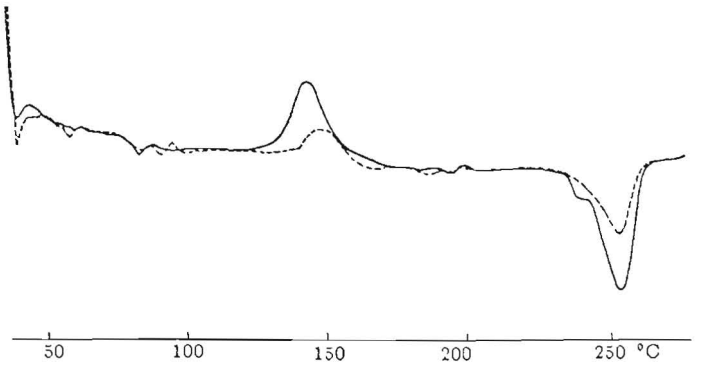

Figure 40. DSC second scan thermograms of PAr/PC/PET with Ultranox 624 and Staboxol P-100 extruded at 300°C (—) and at 325°C (---) [40]

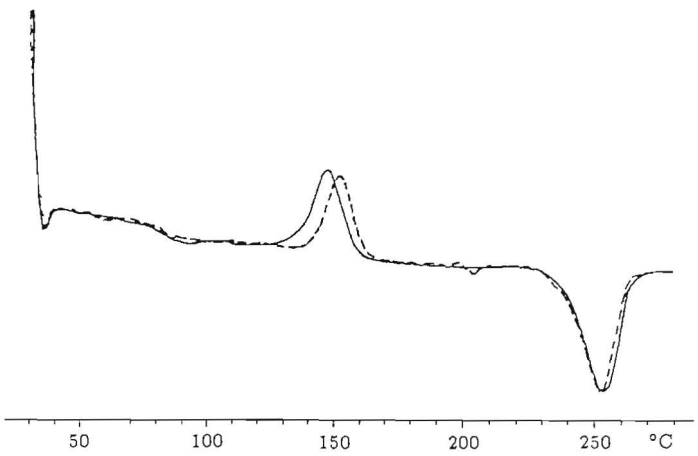

Figure 41. DSC thermograms of PAr/PC/PET with Ultranox 624, Stabaxol P-100 and Ethanox 330, extruded at 325°C: (—) second scan; (---) eighth scan (sample F, Table 3) [40]

the extrusion temperature of 300°C. Upon annealing at 300°C for 30 min, a strong decrease in both ΔH_f and T_m was observed. Addition of Ethanox 330 (hindered phenol) gave a blend which was stable at 300°C for 60 min. Table 3 gives the details of the study on stabilisers.

Cycling experiments can be used effectively to assess the efficiency of the stabiliser combinations [40]. Figure 36 shows the second- and third-cycle thermograms of the blend without stabilisers (extrusion temperature 280°C). It is clear that the third-cycle thermogram shows a decrease in T_m and ΔH_f due to exchange reactions. Figure 37 shows the thermograms of blends stabilised with Ultranox 624. It can be seen that the second-cycle and eighth-cycle thermograms look similar, which indicates stability of the system. The comparison of the second cycle of the sample extruded at 280°C and that at 300°C shows that at 300°C a marked decrease in the cold crystallisation exotherm and the heat of fusion occurs (Figure 38). When another stabiliser, Stabaxol P-100, was also incorporated, even at the extrusion temperature of 300°C the second and the eighth cycles look the same, suggesting a stable system (Figure 39). Again, when the temperature is raised to 325°C the blend shows a decrease in stability (Figure 40). The incorporation of a third component in the stabiliser system imparts stability to the blend as shown by Figure 41.

3.4. *Size-exclusion chromatography*

The reaction mechanism and catalytic behaviour of the various catalysts can be understood from the information of the change in average block lengths with mixing time. In a PC/PET block copolymer the change in block lengths has been studied by size-exclusion chromatography after selective degradation of the PC blocks, leaving the PET blocks unaffected [44,45] (see also Chapter 8).

4. Conclusions

Reactive processing/blending is a very promising technology for preparing new polymeric materials from existing polymers. There is an increasing interest in the understanding of the exchange reactions during reactive processing. The chemical structures and the properties of the resulting polymeric materials are controlled by the relative rate and extent of several reactions occurring during melt-blending. Several analytical techniques have been used which can detect the changes in the chemical structure after reactive processing. The activity of a catalyst, either present as a residue from polymer synthesis or purposely added before blending, may play an important role in controlling the chemical structure of the final product.

Since exchange reactions affect mechanical properties, it is very crucial to control the extent of exchange reactions during melt-blending in order to achieve the desired properties. Organophosphorus compounds, such as phosphites [36,37], phosphonates [38], and phosphates [39], have been used to inhibit ester exchange reactions in the molten state. Lanthanide compounds [44,45] possess a wide range of catalytic activity toward different reactions taking place during PET/PC reactive blending. Hence the choice of the appropriate catalyst is very important to obtain the final product having the desired properties. Reactive blending of condensation polymers has the potential to produce a range of polymer structures from block to multiblock and fully random copolymers. The ability to control structures and sequences in transreactions of condensation polymers offers significant opportunities in creating new properties of well known polymers.

Acknowledgements

One of the authors, Ms. Nirmala James, acknowledges the Council of Scientific and Industrial Research (CSIR), New Delhi, India, for the award of a Senior Research Fellowship.

References

1. L. A. Utracki, "*Polymer Alloys and Blends: Thermodynamics and Rheology*", Hanser Publishers, New York 1990
2. J. A. Manson, L. H. Sperling, "*Polymer Blends and Composites*", Plenum Press, New York 1976
3. C. Beretta, R. A. Weiss, *Am. Chem. Soc. PMSE Prep.* 56, 556 (1987)

4. R. Tannenbaum, M. Rutkowska, A. Eisenberg, *J. Am. Chem. Soc., Polym. Prepr.* **27**, 345 (1986)
5. J. Y. Lee, P. C. Painter, M. M. Coleman, *Macromolecules* **21**, 954 (1988)
6. E. M. Pearce, T. K. Kwei, B. Y. Min, *Am. Chem. Soc. PMSE Prep.* 50, 16 (1984)
7. J. A. Manson, L. H. Sperling, "*Polymer Blends and Composites*", Plenum Press, New York 1976, pp. 87–93
8. M. Xanthos, M. W. Young, J. A. Biesenberger, *Polym. Eng. Sci.* **30**, 355 (1990)
9. K. Kreisher, *Plastics Technol.* **35**, 67 (1989)
10. B. Brown, in: *Reactive Extrusion: Principles and Practice*, edited by M. Xanthos, Hanser Publishers, New York 1992
11. C. Tzoganakis, *Adv. Polym. Technol.* **9**, 321 (1989)
12. M. Xanthos, S. S. Dagli, *Polym. Eng. Sci.* **31**, 929 (1991)
13. R. J. Kumpf, J. S. Wiggins, H. Pielartzik, *Trends Polym. Sci.* **3**, 132 (1995)
14. N. C. Liu, W. E. Baker, *Adv. Polym. Technol.* **11**, 249 (1992)
15. J. R. Campbell, S. Y. Hobbs, T. J. Shea, V. H. Watkins, *Polym. Eng. Sci.* **30**, 1056 (1990)
16. V. J. Triacca, S. Ziaee, J. W. Barlow, H. Keskkhula, D. R. Paul, *Polymer* **32**, 1401 (1991)
17. EP 485834 A2 (1992), Mobay Corp., Inv.: R. J. Kumpf, D. K. Nerger, R. Wehrmann, H. Pielartzik, *Chem. Abstr.* **117**, 172302a (1992)
18. EP 353478 A1 (1990), Dow Chemical Co., Inv.: M. J. Mullins, E. P. Woo, *Chem. Abstr.* **113**, 79270w (1990)
19. R. J. Kumpf, R. Archey, W. Kauthold, A. D. Meltzer, H. Pielartizk, *J. Am. Chem. Soc., Polym. Prepr.* **34**, 580 (1993)
20. S. B. Brown, C. M. Orlando. "*Reactive Extrusion*", in: *Encyclopedia of Polymer Science and Engineering*, 2nd Edition, edited by A. Klingsberg, T. Baldwin, John Wiley and Sons, New York 1988, vol. 14, p. 169
21. A. M. Kotliar, *J. Polym. Sci., Macromol. Rev.* **16**, 367 (1981)
22. P. J. Flory, *Principles of Polymer Chemistry*, Cornell University Press, Ithaca 1953
23. P. J. Flory, *J. Am. Chem. Soc.*, **62**, 1057 (1940)
24. P. J. Flory, *J. Am. Chem. Soc.*, **64**, 2205 (1942)
25. R. Yamadera, M. Murano, *J. Polym. Sci.*, **5A-1**, 2259 (1967)
26. G. della Fortuna, E. Oberrauch, T. Salvatori, E. Sorta, M. Bruzzone, *Polymer* **18**, 269 (1977)
27. US 4417032 (1983), Allied Co., Inv.: Y. P Khanna, E. A. Turi, S. M. Aharoni, T. Largman, *Chem. Abstr.* 100, 52525c (1984)
28. US 4861838 (1989), Allied Signal Inc., Inv.: Y. P. Khanna, *Chem. Abstr.* **112**, 56977x (1990)
29. A. Verma, B. L. Deopura, A. K. Sengupta, *J. Appl. Polym. Sci.* **31**, 747 (1986)
30. J. Devaux, P. Godard, J. P. Mercier, *J. Polym. Sci., Polym. Phys. Ed.* 20, 1901 (1982)
31. M. Kimura, G. Salee, R. S. Porter, *J. Appl. Polym. Sci.* 29, 1629 (1984)
32. P. Godard, J. M. Dekoninck, V. Devlesaver, J. Devaux, *J. Polym. Sci., Part A* **24**, 3301 (1986)

33. K. P. McAlea, J. M. Schultz, K. H. Gardner, G. D. Wignall, *Polymer* **27**, 1581 (1986)
34. I. Mondragon, J. Nazabal, *J. Appl. Polym. Sci.* **32**, 6191 (1986)
35. A. Golovoy, M. F. Cheung, H. van Oene, *Polym. Eng. Sci.* **27**, 1642 (1987)
36. J. Devaux, P. Godard, J. P. Mercier, *Polym. Eng. Sci.* **22**, 229 (1982)
37. US 5646208 (1997), Amoco Corp., Inv.: W. W. Cattron, R. J. Schiavone
38. W. A. Smith, J. W. Barlow, D. R. Paul, *J. Appl. Polym. Sci.* 26, 4233 (1981)
39. FR 2567137 (1986), Rhone-Poulenc Specialities Chimiques, Inv.: Y. Bonin, M. Logeat, *Chem. Abstr.* **105**, 98561t (1986)
40. M. F. Cheung, A. Golovoy, R. O. Carter III, H. van Oene, *Ind. Eng. Chem. Res.* **28**, 476 (1989)
41. Neth. Appl. NL 8602460 (1988), General Electric Co., Inv.: J. J. Verhoeven, *Chem. Abstr.* **109**, 74627a (1988)
42. EP Appl. 295730 A1 (1988), General Electric Co., Inv.: J. J. Verhoeven, W. M. M. Rovers, *Chem. Abstr.* **110**, 174475p (1989)
43. DE 2751969 A1 (1978), Ciba-Geigy, Inv.: J. Habermeier; *Chem. Abstr.* **89**, 1114029 (1978)
44. M. Fiorini, C. Berti, V. Ignatov, M. Toselli, F. Pilati, *J. Appl. Polym. Sci.* **55**, 1157 (1995)
45. M. Fiorini, F. Pilati, C. Berti, M. Toselli, V. Ignatov, *Polymer* **38**, 413 (1997)
46. S. B. Hait, S. Sivaram, *Macromol. Chem. Phys.*, in press
47. L. H. Wang, Z. Huang, T. Hong, R. S. Porter, *J. Macromol. Sci.-Phys.* **B29**, 155 (1990)
48. J. Devaux, P. Godard, J. P. Mercier, R. Touillaux, J. M. Dereppe, *J. Polym. Sci., Polym. Phys. Ed.* **20**, 1881 (1982)
49. Z. H. Huang, L. H. Wang, *Makromol. Chem., Rapid Commun.* **7**, 255 (1986)
50. J. I. Eguiazabal, G. Ucar, M. Cortazar, J. J. Iruin, *Polymer* **27**, 2013 (1986)
51. C. Berti, V. Bonora, F. Pilati, M. Fiorini, *Makromol. Chem.* **193**, 1665 (1992)
52. M. Valero, J. J. Iruin, E. Espinosa, M. J. Fernandez Berridi, *Polym. Commun.* **31**, 127 (1990)
53. K. R. Carduner, R. O. Carter III, M. F. Cheung, A. Golovoy, H. van Oene, *J. Appl. Polym. Sci.* **40**, 963 (1990)
54. M. F. Cheung, K. R. Carduner, A. Golovoy, H. van Oene, *J. Appl. Polym. Sci.* **40**, 977 (1990)
55. A. Golovoy, M. F. Cheung, K. R. Carduner, M. J. Rokosz, *Polym. Eng. Sci.* **29**, 1226 (1989)
56. J. I. Eguiazabal, M. E. Calahorra, M. M. Cortazar, J. J. Iruin, *Polym. Eng. Sci.* **24**, 608 (1984)
57. R. S. Porter, J. M. Jonza, M. Kimura, C. R. Desper, E. R. George, *Polym. Eng. Sci.* **29**, 55 (1989)
58. M. Kimura, R. S. Porter, G. Salee, *J. Polym. Sci., Polym. Phys. Ed.* **21**, 367 (1983)
59. J. S. Kollodge, R. S. Porter, *Polymer* **34**, 4990 (1993)